
CHOOSING THE BEST INTERPOLATION DATA IN IMAGES WITH NOISE

Zakaria BELHACHMI
 IRIMAS
 Université de Haute-Alsace
 Mulhouse, France
 zakaria.belhachmi@uha.fr

Thomas JACUMIN
 IRIMAS
 Université de Haute-Alsace
 Mulhouse, France
 thomas.jacumin@uha.fr

November 5, 2020

ABSTRACT

We introduce and discuss shape based models for finding the best interpolation data in compression of images with noise. The aim is to reconstruct missing regions by means of minimizing data fitting term in the L^2 -norm between the images and their reconstructed counterparts. We analyse the proposed models in the framework of the Γ -convergence from two different points of view. First, we consider a continuous stationary PDE model and get pointwise information on the “relevance” of each pixel by a topological asymptotic method. Second, we introduce a finite dimensional setting into the continuous model based on fat pixels (balls with positive radius), and we study by Γ -convergence the asymptotics when the radius vanishes. We extend the method to time-dependent based reconstruction and discuss several strategies for choosing the interpolation data within masks that might be improved over the iterations. Numerical computations are presented that confirm the usefulness of our theoretical findings for stationary and non-stationary PDE-based image compression.

Keywords image compression · shape optimization · Γ -convergence · image interpolation · inpainting · PDEs · gaussian noise · image denoising · system-aware compression

Introduction

Lossy compression plays a important role in many information systems. Nevertheless, most of these methods do not consider any kind of distortion, called noise, on the source signal to compress. It leads to sub-optimal rate-compression performance. To overcome this issue, Dar and Elad in [1] introduced the concept of “System-Aware Compression”, Figure 1, where the compression methods take care of noises involved by system sensors. For our study, we suppose A and B in Figure 1 to be identity matrices.

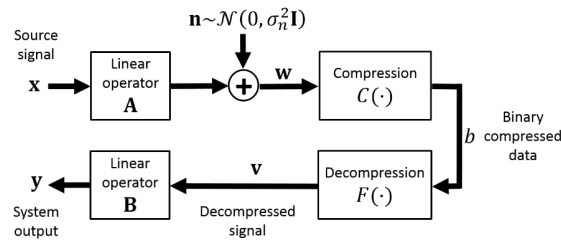


Figure 1: “System-Aware Compression” description from [1].

Using PDEs for image compression is getting more and more interest these past years. However, most of techniques involving PDEs are actually coupled with existing codec such as JPEG [2], JPEG 2000 [3] or wavelet transform [4]. Indeed, PDEs are mainly used as pre-filter or post-filter, for example, for image smoothing or denoising [5, 6, 7, 8]. An interesting idea would be to perform image compression by using a full PDEs-based compression codec [9] by saving a small amount of “important” pixels and interpolate the others by suitable PDEs by using image inpainting from a given set of saved parts of the images [10, 11, 12]. The aim of inpainting is to reconstruct missing parts of the data from known parts, viewed as a Dirichlet boundary condition [13, 14, 15, 16].

Choosing the best interpolation data for image compression, without noise, have been studied in [17] by Belhachmi *et al*, where the aim was to minimize the H^1 semi-norm between the original image and its interpolated counterpart. Their work is the only article that proposes a rigorous mathematical analysis to prove the existence of optimal mask and to provide a way to select such mask. However, because it focuses on edges only, this method gives insufficient results when the input image is affected by noise. Other approaches, mainly stochastic methods have been also proposed [18, 19, 20, 21]. Based only on heuristic arguments, these methods do not consider that optimal sets are dependent on the interpolating PDE. In addition, some ideas based on L^1 minimization play an important role in recent compressed concepts [22].

In this article, we consider the most important pixels that allows us to minimize the L^2 -error between the original image and the interpolated one. This point of view leads to pixels choices that reduce the effect of noise, in particular gaussian noise, and as by product, to perform an amount of simultaneous denoising of the considered images. Moreover, we obtain, in the framework of the Γ -convergence and topological asymptotics, the existence of optimal masks and an effective way to select them. We extend this model to a time-dependent one with two objectifs: first, with a fixed mask, obtained at the initial time, the inpainting yields a denoised image. Second, choosing interpolation data with an adaptive improvement of the mask (which vary in time) allows us to smooth (soften) hard thresholding in the selection and eventually to adjust the size of the mask to a desired accuracy. Numerical experiences, confirm both objectives that is to say an improvement of the inpainting quality and the improvement of the masks during the iterations.

In Section 1, we propose a mathematical model of the problem and its relaxed formulation. In Section 2, we compute the topological gradient of our minimization problem in order to find a mathematical criterion to construct our set of interpolations points. In Section 3, we change our point of view, by considering “fat pixels” instead of a general set of interpolations points. In Section 4, we present a second method which is time dependent when the radius vanishes. We extend the method to time-dependent based reconstruction and discuss several strategies for choosing the interpolation data within masks that might be improved over the iterations. Finally, in Section 5, we expose some numerical results.

1 The Continuous Compression Model

As said previously, we consider that the input signal is affected by gaussian noise. We begin by giving a short review of the gaussian noise model and the “maximum-a-posteriori estimate”.

1.1 Review of the Gaussian Noise Model

We consider the probability space $(\Omega, \mathcal{B}(\mathbb{R}), \mathbb{P})$. In this section, we assimilate the image f as a random vector. We consider a random vector G such that each G_i follows a normal distribution with F_i as mean and σ standard deviation and all G_i are independent. Then, each G_i satisfies

$$\mathbb{P}(G_i | F_i) = \frac{1}{\sigma\sqrt{2\pi}} e^{-\frac{1}{2\sigma^2}(g_i - f_i)^2}.$$

Since every variable is independent, we have

$$\mathbb{P}(G | F) = \prod_{i=0}^N \mathbb{P}(G_i | F_i) = \frac{1}{\sigma\sqrt{2\pi}} e^{-\frac{1}{2\sigma^2} \sum_{i=0}^N (g_i - f_i)^2} = \frac{1}{\sigma\sqrt{2\pi}} e^{-\frac{1}{2\sigma^2} \|g - f\|_2^2}.$$

For denoising purpose, we generally use the “maximum-a-posteriori estimate” [23, 24] of $f = (f_i)_{i=1}^N$ in \mathbb{R}^N for a given g in \mathbb{R}^N , that is

$$\max_{f \in \mathbb{R}^N} \mathbb{P}(F = f \mid G = g),$$

or equivalently

$$\max_{f \in \mathbb{R}^N} \ln \mathbb{P}(F \mid G).$$

By using Bayes formula, we get

$$\begin{aligned} \max_{f \in \mathbb{R}^N} \ln \mathbb{P}(F \mid G) &= \max_{f \in \mathbb{R}^N} \ln \frac{\mathbb{P}(F) \mathbb{P}(G \mid F)}{\mathbb{P}(G)} \\ &= \max_{f \in \mathbb{R}^N} \ln \mathbb{P}(F) + \ln \mathbb{P}(G \mid F) - \ln \mathbb{P}(G). \end{aligned}$$

Since $\mathbb{P}(G)$ does not depend on f , we obtain

$$\max_{f \in \mathbb{R}^N} \mathbb{P}(F \mid G) \Leftrightarrow \min_{f \in \mathbb{R}^N} \frac{1}{2\sigma^2} \|g - f\|_2^2 + \ln \mathbb{P}(F).$$

We call $\mathbb{P}(F)$ the prior on images. If we consider a uniform prior on images with normalized intensity values, which is $\mathbb{P}(F_i = f_i) = 1$ if $0 \leq f_i \leq 1$ and 0 otherwise, we have that the maximum-a-posteriori estimate of F is equivalent to

$$\min_{f \in [0,1]^N} \|g - f\|_2^2.$$

This result shows us that, minimizing the L^2 -error is equivalent as removing gaussian noise. As a result, we focus our study on the L^2 -error in the sequel.

1.2 The Compression Model

From this point, we want to minimize the L^2 -error between the noised input signal and the recovered signal. Actually, we do not minimize the L^2 -error, but a Tikhonov regularized [25] L^2 -error, that we denote by J in the sequel. We begin by giving a mathematical model of the problem. Let D be a smooth bounded open subset of \mathbb{R}^2 . We study for, $\alpha > 0$, the problem

Problem 1.1. Find u in $H^1(D)$ such that

$$\begin{cases} -\alpha \Delta u + u = 0, & \text{in } D \setminus K, \\ u = f, & \text{in } K, \\ \frac{\partial u}{\partial \mathbf{n}} = 0 & \text{on } \partial D. \end{cases} \quad (1)$$

It is well known that if $u_K \in H^1(D)$ is a solution of Problem 1.1, then u_K is a minimizer of

$$\min \left\{ \frac{\alpha}{2} \int_D |\nabla u|^2 dx + \frac{1}{2} \int_D u^2 dx \mid u \in H^1(D), u = f \text{ a.e. on } K \right\}. \quad (2)$$

The shape optimization problem we study is

$$\min_{K \subseteq D, m(K) \leq c} \{J(u_K) \mid u_K \text{ solution of Problem 1.1}\}, \quad (3)$$

where J , defined by

$$J(u) = \frac{1}{2} \int_D (u - f)^2 dx + \frac{\alpha}{2} \int_D |\nabla u - \nabla f|^2 dx, \quad (4)$$

is called the cost functional, m is a given measure and $c > 0$. In fact, the cost functional we choose to study is the L^2 -norm with a regularization term characterized by α .

1.2.1 Reformulation

In this section, we want to give a max-min formulation of the optimization problem (3). This new formulation will be more convenient to use later. We have the following proposition :

Proposition 1.1. *The optimization problem (3) is equivalent to*

$$\max_{K \subseteq D, m(K) \leq c} \min_{u \in H^1(D), u=f \text{ in } K} \frac{\alpha}{2} \int_D |\nabla u|^2 dx + \frac{1}{2} \int_D u^2 dx.$$

Proof. Let u_K be a solution of Problem 1.1. Thus,

$$\begin{aligned} (3) &\Leftrightarrow \min_{K \subseteq D} \frac{1}{2} \int_D (u_K - f)^2 dx + \frac{\alpha}{2} \int_D |\nabla u_K - \nabla f|^2 dx \\ &\Leftrightarrow \min_{K \subseteq D} \frac{1}{2} \int_D u_K^2 dx + \frac{\alpha}{2} \int_D |\nabla u_K|^2 dx - \int_D u_K f dx - \alpha \int_D \nabla u_K \cdot \nabla f dx. \end{aligned}$$

The weak formulation of Problem 1.1 gives us $\alpha \int_D \nabla u_K \cdot \nabla f dx = \int_D u_K^2 dx + \alpha \int_D |\nabla u_K|^2 dx - \int_D u_K f dx$. Hence,

$$\begin{aligned} (3) &\Leftrightarrow \min_{K \subseteq D} \frac{1}{2} \int_D u_K^2 dx + \frac{\alpha}{2} \int_D |\nabla u_K|^2 dx - \int_D u_K f dx - \int_D u_K^2 dx - \alpha \int_D |\nabla u_K|^2 dx + \int_D u_K f dx \\ &\Leftrightarrow \min_{K \subseteq D} -\frac{1}{2} \int_D u_K^2 dx - \frac{\alpha}{2} \int_D |\nabla u_K|^2 dx \\ &\Leftrightarrow \max_{K \subseteq D} \frac{\alpha}{2} \int_D |\nabla u_K|^2 dx + \frac{1}{2} \int_D u_K^2 dx. \end{aligned}$$

Using (2), we get the result. \square

Remark. The new formulation of our optimization problem (3) can be rewritten by penalizing the measure constraint on K as follow :

$$\max_{K \subseteq D} \min_{u \in H^1(D), u=f \text{ in } K} \frac{\alpha}{2} \int_D |\nabla u|^2 dx + \frac{1}{2} \int_D u^2 dx - \beta m(K), \quad (5)$$

for $\beta > 0$.

The well-posedness of (3) depends of the choice of the measure m . In [17], it has been proven that, in the Laplacian case, choosing the ν -capacity as measure m leads to the well-posedness of the optimization problem. Consequently, we will study (3) when m is the ν -capacity.

1.2.2 Framework of the γ -convergence

For the sake of completeness we recall the definition of the ν -capacity, for $\nu > 0$, Γ -convergence and γ -convergence written in [17]. More details about the ν -capacity or the shape optimization tools can be found in [26, 27]. Let us start with some definitions.

Definition 1.1 (ν -capacity of a set). *Let $V \subseteq \mathbb{R}^d$ be a smooth bounded open set and $\nu > 0$. We define the ν -capacity of a subset E in V by*

$$\text{cap}_\nu(E, V) = \inf \left\{ \int_V |\nabla u|^2 dx + \nu \int_V u^2 dx \mid u \in H_0^1(V), u \geq 1 \text{ a.e. in } E \right\}.$$

Remark. We notice that if, for a given set $E \subseteq V$ and $\nu > 0$, we have $\text{cap}_\nu(E, V) = 0$, then we have $\text{cap}_\nu(E, V) = 0$ for every $\nu > 0$. Thus, the sets of vanishing capacity are the same for all $\nu > 0$. That is why we will drop the ν and simply write cap instead of cap_ν .

Definition 1.2 (quasi-everywhere property). We say that property holds **quasi-everywhere** if it holds for all x in E except for the elements of a set Z subset of E such that $\text{cap}(Z, E) = 0$. We write q.e.

Definition 1.3 (quasi-open set). We say that a subset A of E is **quasi-open** if for every $\varepsilon > 0$ there exists an open subset A_ε of D , such that $A \subseteq A_\varepsilon$ and $\text{cap}(A_\varepsilon \setminus A, D) < \varepsilon$.

We introduce the set $\mathcal{M}_0(D)$ which is denoted by $\mathcal{M}_0^*(D)$ in [28]

Definition 1.4 (The set $\mathcal{M}_0(D)$). We denote by $\mathcal{M}_0(D)$ the set of all non negative Borel measures μ on D , such that

- $\mu(B) = 0$, for every Borel set B subset of D with $\text{cap}(B, D) = 0$,
- $\mu(B) = \inf \{ \mu(U) \mid U \text{ quasi-open, } B \subseteq U \}$, for every Borel subset B of D .

Definition 1.5 (ν -capacity of a measure). The ν -capacity, for $\nu > 0$, of a measure μ of $\mathcal{M}_0(D)$ is defined by

$$\text{cap}_\nu(\mu, D) := \inf_{u \in H_0^1(D)} \int_D |\nabla u|^2 dx + \nu \int_D u^2 dx + \int_D (u-1)^2 d\mu.$$

The next proposition will gives us a natural way to identify a set to a measure of $\mathcal{M}_0(D)$.

Proposition 1.2. Let E be a Borel subset of D . We denote by ∞_E the measure of $\mathcal{M}_0(D)$ defined by

$$\infty_E(B) := \begin{cases} +\infty & , \text{ if } \text{cap}(B, D) > 0, \\ 0 & , \text{ otherwise.} \end{cases}, \text{ for all } B \text{ Borel subset of } D.$$

Remark. For a given Borel subset E of D , we have $\text{cap}_\nu(\infty_E, D) = \text{cap}_\nu(E, D)$.

Definition 1.6 (Γ -convergence). Let V be a topological space. We say that the sequence of functionals $(F_n)_n$, from V into \mathbb{R} , Γ -converges to F in V if

- for every u in V , there exists a sequence $(u_n)_n$ in V such that $u_n \rightarrow u$ in V and $F(u) \geq \limsup_{n \rightarrow +\infty} F_n(u_n)$,
- for every sequence $(u_n)_n$ in V such that $u_n \rightarrow u$ in V , we have $F(u) \leq \liminf_{n \rightarrow +\infty} F_n(u_n)$.

We write sometimes $\Gamma - \lim_{n \rightarrow +\infty} F_n = F$.

Definition 1.7 (γ -convergence). We say that a sequence $(\mu_n)_n$ of measures in $\mathcal{M}_0(D)$ γ -converge to a measure μ in $\mathcal{M}_0(D)$ with respect to F (or $(\mu_n)_n$ $\gamma(F)$ -converge to μ) if F_{μ_n} Γ -converge in $L^2(D)$ to F_μ .

We give a locality of the γ -convergence result, then the γ -compactity of $\mathcal{M}_0(D)$, from [29] and [28] respectively.

Proposition 1.3 (Locality of the γ -convergence). Let $(\mu_n^1)_n$ and $(\mu_n^2)_n$ be two sequences of measures in $\mathcal{M}_0(D)$ which $\gamma(F)$ -converge to μ^1 and μ^2 respectively. Assume that μ_n^1 and μ_n^2 coincide q.e. on a subset D' of D , for every $n \in \mathbb{N}$. Then μ^1 and μ^2 coincide q.e. on D' .

Proposition 1.4 (γ -compactity of $\mathcal{M}_0(D)$). The set $\mathcal{M}_0(D)$ is compact with respect to the γ -convergence. Moreover, the class of measures of the form $\infty_{D \setminus A}$, with A open and smooth subset of D , is dense in $\mathcal{M}_0(D)$.

Remark. The result above means that, for every μ in $\mathcal{M}_0(D)$, there exists a family of subsets $(E_n)_n$ of D , such that ∞_{E_n} γ -converge to μ .

We will use in the sequel the shape analysis tools that we introduced in this section, in order to study the optimization problem (3).

1.2.3 Analysis

Now, let us come back to our problem. Thanks to Proposition 1.1, our optimization problem (7) can be rewritten by penalizing the Dirichlet boundary condition $u = f$ in K and penalizing the constraint $\text{cap}(K) \leq c$ as follow

$$\max_{K \subseteq D} \min_{u \in H^1(D)} \frac{\alpha}{2} \int_D |\nabla u|^2 dx + \frac{1}{2} \int_D u^2 dx + \frac{1}{2} \int_D (u - f)^2 d\infty_K - \beta \text{cap}(\infty_K),$$

where $\beta > 0$ depends on c . The term $\int_D (u - f)^2 d\infty_K$ ensure us that u is equals to f in K while the term $-\beta \text{cap}(\infty_K)$ penalize the constraint $\text{cap}(K) \leq c$. Since the optimization problem over K with this kind of problem does not always a solution, we proceed to a relaxation process. We want to study the optimization problem below that we claim is the relaxed problem of the previous problem

$$\max_{\mu \in \mathcal{M}_0(D)} \min_{u \in H^1(D)} \frac{\alpha}{2} \int_D |\nabla u|^2 dx + \frac{1}{2} \int_D u^2 dx + \frac{1}{2} \int_D (u - f)^2 d\mu - \beta \text{cap}(\mu),$$

where μ is in $\mathcal{M}_0(D)$. Here we do not want μ to simply be a characteristic function since a family of characteristic functions does not always converge to a characteristic function, which will be important later. For every μ in $\mathcal{M}_0(D)$ and u in $H^1(D)$, we define F_μ , from $H^1(D)$ into $\mathbb{R} \cup \{+\infty\}$, by

$$F_\mu(u) := \begin{cases} \alpha \int_D |\nabla u|^2 dx + \int_D u^2 dx + \int_D (u - f)^2 d\mu & , \text{ if } |u| \leq |f|_\infty, \\ +\infty & , \text{ otherwise.} \end{cases}$$

We have that F_μ is equicoercive with respect to μ , for any μ in $\mathcal{M}_0(D)$. Indeed, let u be in $H^1(D)$ such that $|u| \leq |f|_\infty$,

$$\begin{aligned} F_\mu(u) &= \alpha \int_D |\nabla u|^2 dx + \int_D u^2 dx + \int_D (u - f)^2 d\mu \\ &= \alpha \int_D |\nabla u|^2 dx + \int_D u^2 dx + \int_D u^2 d\mu + \int_D f^2 d\mu - 2 \int_D u f d\mu \\ &\geq \alpha \int_D |\nabla u|^2 dx + \int_D u^2 dx - 2 \int_D u f d\mu \\ &\geq \alpha \int_D |\nabla u|^2 dx + \int_D u^2 dx - 2|u|_\infty |f|_\infty \mu(D) \\ &\geq \alpha \int_D |\nabla u|^2 dx + \int_D u^2 dx - 2|f|_\infty^2 \mu(D). \end{aligned}$$

For every μ in $\mathcal{M}_0(D)$, we define E , from $\mathcal{M}_0(D)$ into \mathbb{R} , by

$$E(\mu) := \min_{u \in H^1(D)} F_\mu(u) = \min_{u \in H^1(D)} \alpha \int_D |\nabla u|^2 dx + \int_D u^2 dx + \int_D (u - f)^2 d\mu.$$

For a given μ in $\mathcal{M}_0(D)$, $E(\mu)$ correspond to the energy of

Problem 1.2. Find u in $H^1(D)$ such that

$$\begin{cases} -\alpha \Delta u + u + \mu(u - f) = 0, & \text{in } D, \\ \frac{\partial u}{\partial \mathbf{n}} = 0, & \text{on } \partial D. \end{cases} \quad (6)$$

Thus, if u is a solution of Problem 1.2 for a given μ in $\mathcal{M}_0(D)$, then $F_\mu(u) = E(\mu)$ and u satisfied the maximum principle $|u| \leq |f|_\infty$. Since we want to include balls centering in x_0 in D , we do not want x_0 to be too close to the boundary of D . That is why, we introduce the following notations for $\delta > 0$,

$$D^{-\delta} := \{x \in D \mid d(x, \partial D) \geq \delta\} \subseteq D,$$

$$\mathcal{K}^\delta(D) := \{K \subseteq D \mid K \text{ closed, } K \subseteq D^{-\delta}\},$$

and

$$\mathcal{M}_0^\delta(D) := \{\mu \in \mathcal{M}_0(D) \mid \mu|_{D \setminus D^{-\delta}} = 0\} \subseteq \mathcal{M}_0(D).$$

The problem we study now is the following

$$\max_{\mu \in \mathcal{M}_0^\delta(D)} \min_{u \in H^1(D)} \frac{\alpha}{2} \int_D |\nabla u|^2 dx + \frac{1}{2} \int_D u^2 dx + \frac{1}{2} \int_D (u - f)^2 d\mu - \beta \text{cap}(\mu).$$

Using the γ -compactness of $\mathcal{M}_0(D)$, Proposition 1.4 and the locality of the $\gamma(F)$ -convergence, Proposition 1.3, we have the result below.

Proposition 1.5 (γ -compactness of $\mathcal{M}_0^\delta(D)$). *The set $\mathcal{M}_0^\delta(D)$ defined above is compact with respect to the γ -convergence.*

We have the following theorem

Theorem 1.1. *We have*

$$\text{cl}_\gamma \mathcal{K}_\delta(D) = \mathcal{M}_0^\delta(D),$$

i.e. $\mathcal{K}_\delta(D)$ is dense into $\mathcal{M}_0^\delta(D)$ with respect to the $\gamma(F)$ -convergence.

Proof. For every K in $\mathcal{K}_\delta(D)$, we have $K \subset D$. Thus ∞_K is in $\mathcal{M}_0^\delta(D)$, so $\mathcal{K}_\delta(D) \subseteq \mathcal{M}_0^\delta(D)$ if we identify a set of $\mathcal{K}_\delta(D)$ by its measure. By the γ -compactness of $\mathcal{M}_0^\delta(D)$, see Proposition 1.5, we have $\text{cl}_\gamma \mathcal{K}_\delta(D) \subseteq \mathcal{M}_0^\delta(D)$.

Conversely, let μ be in $\mathcal{M}_0^\delta(D)$. We need to prove that μ is in $\text{cl}_\gamma \mathcal{K}_\delta(D)$ i.e. μ is the γ -limit of elements of $\mathcal{K}_\delta(D)$. This is to be understood as, there exist elements $(K_n)_n$ of $\mathcal{K}_\delta(D)$ such that, ∞_{K_n} γ -converge to μ . Since $\mathcal{M}_0(D)$ is dense and $\mathcal{M}_0^\delta(D) \subset \mathcal{M}_0(D)$, we know that there exists a sequence $(K_n)_n$ of $\mathcal{P}(D)$ such that, ∞_{K_n} γ -converge to μ . We need to show that K_n are in $\mathcal{K}_\delta(D)$. By the locality property of the γ -convergence (Proposition 1.3), we can choose $(K_n)_n$ such that $K_n \subseteq (D^{-\delta})^{1/n}$. Making a homothety $\varepsilon_n K_n$, for $\varepsilon_n < 0$ such that $\varepsilon_n K_n \subseteq D^{-\delta}$, we have $\varepsilon_n K_n \in \mathcal{K}_\delta(D)$. Moreover, we can choose ε_n such that $\varepsilon_n \rightarrow 1$, therefore $\varepsilon_n K_n$ γ -converge to μ . \square

Similarly to Lemma 3.4 in [17], we have

Theorem 1.2. *Let $\mu_n \in \mathcal{K}_\delta(D)$. If μ_n γ -converge to μ , then $\text{cap}_\nu(\mu_n) \rightarrow \text{cap}_\nu(\mu)$.*

Theorem 1.3. *If $(\mu_n)_n$ in $\mathcal{M}_0^\delta(D)$ γ -converges to μ , then μ is in $\mathcal{M}_0^\delta(D)$ and F_{μ_n} Γ -converges to F_μ in $L^2(D)$.*

Proof. This proof is similar to the one of Theorem 3.5 in [17]. We suppose that $(\mu_n)_n$ in $\mathcal{M}_0^\delta(D)$ γ -converges to μ . By γ -compactness, Proposition 1.5, μ is in $\mathcal{M}_0^\delta(D)$. Now we prove F_{μ_n} Γ -converges to F_μ in $L^2(D)$.

• **lim inf :** Let $(u_n)_n$ be a sequence in $H^1(D)$ which converge in $L^2(D)$ to u . Let $\varphi \in C_c^\infty(D)$, $0 \leq \varphi \leq 1$ and $\varphi = 1$ in $D^{-\delta}$. Then $(u_n \varphi)_n$ is a sequence in $H^1(D^{-\delta})$ and $u_n \varphi \rightarrow_{n \rightarrow +\infty} u \varphi$ in $L^2(D)$. Since $(\mu_n)_n$ $\gamma(F)$ -converges to μ , we have, in particular for $(\mu_n)_n$,

$$\liminf_{n \rightarrow +\infty} F_{\mu_n}(u_n \varphi) \geq F_\mu(u \varphi)$$

i.e.

$$\liminf_{n \rightarrow +\infty} \left(\alpha \int_D |\nabla(u_n \varphi)|^2 dx + \int_D u_n^2 \varphi^2 dx + \int_D (u_n \varphi - f)^2 d\mu_n \right) \geq \alpha \int_D |\nabla(u \varphi)|^2 dx + \int_D u^2 \varphi^2 dx + \int_D (u \varphi - f)^2 d\mu.$$

By developping,

$$\begin{aligned} & \liminf_{n \rightarrow +\infty} \left(\alpha \int_D |\varphi \nabla u_n|^2 dx + \alpha \int_D |u_n \nabla \varphi|^2 dx + 2\alpha \int_D u_n \varphi \nabla u_n \cdot \nabla \varphi dx + \int_D u_n^2 \varphi^2 dx + \int_D (u_n \varphi - f)^2 d\mu_n \right) \\ & \geq \alpha \int_D |\varphi \nabla u|^2 dx + \alpha \int_D |u \nabla \varphi|^2 dx + 2\alpha \int_D u \varphi \nabla u \cdot \nabla \varphi dx + \int_D u^2 \varphi^2 dx + \int_D (u \varphi - f)^2 d\mu. \end{aligned}$$

Eliminating the converging terms, except $\int_D u_n^2 \varphi^2 dx$ and $\int_D u^2 \varphi^2 dx$, we get

$$\liminf_{n \rightarrow +\infty} \left(\alpha \int_D |\varphi \nabla u_n|^2 dx + \int_D u_n^2 \varphi^2 dx + \int_D (u_n \varphi - f)^2 d\mu_n \right) \geq \alpha \int_D |\varphi \nabla u|^2 dx + \int_D u^2 \varphi^2 dx + \int_D (u \varphi - f)^2 d\mu.$$

In the left hand side, we use that $0 \leq \varphi \leq 1$, and in the right hand side, we take the supremum over all admissible φ , since the inequality above is true for all φ ,

$$\liminf_{n \rightarrow +\infty} \left(\alpha \int_D |\nabla u_n|^2 dx + \int_D u_n^2 dx + \int_D (u_n - f)^2 d\mu_n \right) \geq \sup_{\varphi} \left(\alpha \int_D |\varphi \nabla u|^2 dx + \int_D u^2 \varphi^2 dx + \int_D (u \varphi - f)^2 d\mu \right).$$

Since μ is equals to 0 in $D \setminus D^{-\delta}$, we have

$$\liminf_{n \rightarrow +\infty} \left(\alpha \int_D |\nabla u_n|^2 dx + \int_D u_n^2 dx + \int_D (u_n - f)^2 d\mu_n \right) \geq \sup_{\varphi} \left(\alpha \int_D |\nabla u|^2 \varphi^2 dx + \int_D u^2 \varphi^2 dx \right) + \int_D (u - f)^2 d\mu.$$

We get the lim inf inequality.

• **lim sup :** Let u be in $H^1(D)$, such that the principle maximum is fulfilled, i.e. $|u| \leq |f|_{\infty}$, and \tilde{u} be the extension of u in $H_0^1(D^\delta)$, where D^δ is the dilatation by a factor δ of D . By the locality property of the γ -convergence, Property 1.3, we have that μ_n γ -converge to $\mu(G)$ in D^δ , where G is

$$G_\mu(u) = \int_D |\nabla u|^2 dx + \int_D u^2 dx + \varepsilon \int_{D^\delta \setminus D} |\nabla u|^2 dx + \varepsilon \int_{D^\delta \setminus D} u^2 dx + \int_D (u - f)^2 d\mu,$$

for $\varepsilon > 0$. Hence, there exists a sequence $(u_n^\varepsilon)_n$ of $H_0^1(D^\delta)$ such that u_n^ε converge to \tilde{u} in $L^2(D^\delta)$ and $G_\mu(\tilde{u}) \geq \limsup_{n \rightarrow +\infty} G_{\mu_n}(u_n^\varepsilon)$ i.e.

$$\begin{aligned} & \int_D |\nabla \tilde{u}|^2 dx + \int_D \tilde{u}^2 dx + \varepsilon \int_{D^\delta \setminus D} |\nabla \tilde{u}|^2 dx + \varepsilon \int_{D^\delta \setminus D} \tilde{u}^2 dx + \int_D (\tilde{u} - f)^2 d\mu \\ & \geq \limsup_{n \rightarrow +\infty} \int_D |\nabla u_n^\varepsilon|^2 dx + \int_D (u_n^\varepsilon)^2 dx + \varepsilon \int_{D^\delta \setminus D} |\nabla u_n^\varepsilon|^2 dx + \varepsilon \int_{D^\delta \setminus D} (u_n^\varepsilon)^2 dx + \int_D (u_n^\varepsilon - f)^2 d\mu_n. \end{aligned}$$

Thus, we have

$$\begin{aligned} & \int_D |\nabla \tilde{u}|^2 dx + \int_D \tilde{u}^2 dx + \varepsilon \int_{D^\delta \setminus D} |\nabla \tilde{u}|^2 dx + \varepsilon \int_{D^\delta \setminus D} \tilde{u}^2 dx + \int_D (\tilde{u} - f)^2 d\mu \\ & \geq \limsup_{n \rightarrow +\infty} \int_D |\nabla u_n^\varepsilon|^2 dx + \int_D (u_n^\varepsilon)^2 dx + \int_D (u_n^\varepsilon - f)^2 d\mu_n. \end{aligned}$$

Since \tilde{u} is fixed, we make ε tends to 0 and extract by a diagonal procedure a subsequence $u_n^{\varepsilon_n}$ converging in $L^2(D^\delta)$ to \tilde{u} i.e.

$$\int_D |\nabla \tilde{u}|^2 dx + \int_D \tilde{u}^2 dx + \int_D (\tilde{u} - f)^2 d\mu \geq \limsup_{n \rightarrow +\infty} \int_D |\nabla u_n^{\varepsilon_n}|^2 dx + \int_D (u_n^{\varepsilon_n})^2 dx + \int_D (u_n^{\varepsilon_n} - f)^2 d\mu_n.$$

Setting $u_n := u_n^{\varepsilon_n}|_D \in H^1(D)$, we have since $u = \tilde{u}|_D$,

$$\int_D |\nabla u|^2 dx + \int_D u^2 dx + \int_D (u - f)^2 d\mu \geq \limsup_{n \rightarrow +\infty} \int_D |\nabla u_n|^2 dx + \int_D (u_n)^2 dx + \int_D (u_n - f)^2 d\mu_n.$$

□

Finally, here is the main result of this section.

Theorem 1.4. *We have*

$$\sup_{K \in \mathcal{K}_\delta(D)} (E(\infty_K) - \beta \text{cap}_\nu(\infty_K)) = \max_{\mu \in \mathcal{M}_0^\delta(D)} (E(\mu) - \beta \text{cap}_\nu(\mu)).$$

Proof. Let $(K_n)_n \subset \mathcal{K}_\delta(D)$ be a maximizing sequence of $E(\infty_K) - \beta \text{cap}_\nu(\infty_K)$ i.e.

$$\lim_{n \rightarrow +\infty} E(\infty_{K_n}) - \beta \text{cap}_\nu(\infty_{K_n}) = \sup_{K \in \mathcal{K}_\delta(D)} (E(\infty_K) - \beta \text{cap}_\nu(\infty_K)).$$

One can extract, since $\mathcal{M}_0^\delta(D)$ is a compact metric space when endowed with the distance d_γ (Proposition 1.5), from $(\infty_{K_n})_n \subset \mathcal{M}_0^\delta(D)$ a γ -convergent subsequence. We denote by μ_{lim} this γ -limit. We know that μ_{lim} is in $\mathcal{M}_0^\delta(D)$ since $\mathcal{M}_0^\delta(D)$ is dense with respect to the γ -convergence (Proposition 1.5). We denote by $G(\mu_{\text{lim}})$ the value

$$G(\mu_{\text{lim}}) := \lim_{n \rightarrow +\infty} E(\infty_{K_n}) - \beta \text{cap}_\nu(\infty_{K_n}).$$

By definition of the γ -convergence, we have $\Gamma - \lim_{n \rightarrow +\infty} F_{\infty_{K_n}} = F_{\mu_{\text{lim}}}$. Since $F_{\infty_{K_n}}$ is equicoercive, we can apply Theorem 7.8 in [26]. It leads

$$E(\mu_{\text{lim}}) := \min_{u \in H^1(D)} F_{\mu_{\text{lim}}}(u) = \lim_{n \rightarrow +\infty} \inf_{u \in H^1(D)} F_{\infty_{K_n}}(u) =: \lim_{n \rightarrow +\infty} E(\infty_{K_n}).$$

In addition, by Theorem 1.3 and unicity of the limit, we have

$$\lim_{n \rightarrow +\infty} E(\infty_{K_n}) - \beta \text{cap}_\nu(\infty_{K_n}) = G(\mu_{\text{lim}}) = E(\mu_{\text{lim}}) - \beta \text{cap}_\nu(\mu_{\text{lim}}).$$

Thus, we have

$$\begin{aligned} \sup_{K \in \mathcal{K}_\delta(D)} (E(\infty_K) - \beta \text{cap}_\nu(\infty_K)) &= \lim_{n \rightarrow +\infty} E(\infty_{K_n}) - \beta \text{cap}_\nu(\infty_{K_n}) = E(\mu_{\text{lim}}) - \beta \text{cap}_\nu(\mu_{\text{lim}}) \\ &= \max_{\mu \in \mathcal{M}_0^\delta(D)} (E(\mu) - \beta \text{cap}_\nu(\mu)). \end{aligned}$$

□

Remark. The result above gives us the following information : for every maximizing sequence of sets in $\mathcal{K}_\delta(D)$ of

$$\min_{u \in H^1(D)} \alpha \int_D |\nabla u|^2 dx + \int_D u^2 dx + \int_D (u - f)^2 d\infty_K - \beta \text{cap}_\nu(\infty_K),$$

which corresponds to our original shape optimization problem (3) where m is the capacity, one can extract a converging subsequence which is the solution of the relaxed problem

$$\max_{\mu \in \mathcal{M}_0^\delta(D)} \min_{u \in H^1(D)} \alpha \int_D |\nabla u|^2 dx + \int_D u^2 dx + \int_D (u - f)^2 d\mu - \beta \text{cap}_\nu(\mu).$$

In the next two sections, we aim to find a way to construct the optimal set K .

2 Topological Gradient

Here, we aim to compute the solution of our optimization problem (3) by using a topological gradient based algorithm as in [30, 31]. This kind of algorithm consists in starting with $K = \bar{D}$ and determine how making small holes in K affect the cost functional, in order to find the balls which have the most decreasing effect. To this end, let us define K_ε the compact set $K \setminus B(x_0, \varepsilon)$ where $B(x_0, \varepsilon)$ is the ball centered in $x_0 \in D$ with radius $\varepsilon > 0$ such that $B(x_0, \varepsilon) \subset K$. Let us denote by j the functional

$$j : A \in \mathcal{P}(D) \mapsto \min_{u \in H^1(D), u=f \text{ in } A} \frac{\alpha}{2} \int_D |\nabla u|^2 dx + \frac{1}{2} \int_D u^2 dx.$$

Finally, we denote by u_ε the minimizer of $j(K_\varepsilon)$. Then, we have

Proposition 2.1. *With notations from above, we have when ε tends to 0,*

$$j(K_\varepsilon) - j(K) = (f(x_0) - \alpha \Delta f(x_0))^2 \pi \varepsilon^4 \ln(\varepsilon) + O(\varepsilon^4).$$

Proof.

$$j(K_\varepsilon) - j(K) = \frac{\alpha}{2} \int_{B(x_0, \varepsilon)} |\nabla u_\varepsilon|^2 dx + \frac{1}{2} \int_{B(x_0, \varepsilon)} u_\varepsilon^2 dx - \frac{\alpha}{2} \int_{B(x_0, \varepsilon)} |\nabla f|^2 dx - \frac{1}{2} \int_{B(x_0, \varepsilon)} f^2 dx.$$

The weak formulation of Problem 1.1 leads to

$$j(K_\varepsilon) - j(K) = \frac{\alpha}{2} \int_{B(x_0, \varepsilon)} \nabla u_\varepsilon \cdot \nabla f dx + \frac{1}{2} \int_{B(x_0, \varepsilon)} u_\varepsilon f dx - \frac{\alpha}{2} \int_{B(x_0, \varepsilon)} |\nabla f|^2 dx - \frac{1}{2} \int_{B(x_0, \varepsilon)} f^2 dx.$$

Thus

$$\begin{aligned} j(K_\varepsilon) - j(K) &= \frac{\alpha}{2} \int_{B(x_0, \varepsilon)} \nabla(u_\varepsilon - f) \cdot \nabla f dx + \frac{1}{2} \int_{B(x_0, \varepsilon)} (u_\varepsilon - f) f dx \\ &= -\frac{\alpha}{2} \int_{B(x_0, \varepsilon)} (u_\varepsilon - f) \Delta f dx + \frac{1}{2} \int_{B(x_0, \varepsilon)} (u_\varepsilon - f) f dx \\ &= \frac{1}{2} \int_{B(x_0, \varepsilon)} (u_\varepsilon - f) (f - \alpha \Delta f) dx \end{aligned}$$

We have $(f - \alpha \Delta f(x)) = (f - \alpha \Delta f)(x_0) + \|x - x_0\|O(1)$, and hence

$$j(K_\varepsilon) - j(K) = (f - \alpha \Delta f)(x_0) \int_{B(x_0, \varepsilon)} u_\varepsilon - f dx + \varepsilon O(1) \int_{B(x_0, \varepsilon)} u_\varepsilon - f dx.$$

It is enough to compute the fundamental term in the asymptotic development of the expression $\int_{B(x_0, \varepsilon)} u_\varepsilon - f dx$. This is done by using Proposition B.1 with $w = u_\varepsilon - f$ and $g = -f + \alpha \Delta f$. \square

Since for $\varepsilon < 1$, $\ln \varepsilon < 0$, the result above suggests to keep the points x_0 where $(f - \alpha \Delta f(x_0))^2$ is maximal, when ε small enough. From a practical point of view, this is the main result of our local shape analysis. In the next section, we will see that such strict threshold rule might be relaxed.

The filter $f - \alpha \Delta f$ is known in image enhancement as a basic filter for image enhancement. It aims to produce more contrasted images. In [17], the use of the H^1 -semi-norm gives more importance to the laplacian of f , and the criterion leads to select only the pixels close to the edges. In our approach, it appears that on one side also pixels ‘‘far’’ from the edges may be selected and the neighborhood of the edges is more efficiently restricted with the image enhancement.

The mask creation involve the computation of Δf , which is very sensitive to noise. That is why it is better in practice to smooth the image f before to reduce image noise.

3 Optimal Distribution of Pixels : The ‘‘Fat Pixels’’ Approach

In this section, we change our point of view, by considering ‘‘fat pixels’’ instead of a general set of interpolation points. In the sequel, we will follow [17, 32]. We restrict our class of admissible sets as an union of balls which represent pixels. For $m > 0$ and $n \in \mathbb{N}$, we define

$$\mathcal{A}_{m,n} := \left\{ \bar{D} \cap \bigcup_{i=1}^n \overline{B(x_i, r)} \mid x_i \in D_r, r = mn^{-1/2} \right\},$$

where D_r is the r -neighbourhood of D . The following analysis remains unchanged in \mathbb{R}^d , but for the sake of simplicity we restrict ourself to the case $d = 2$. We consider problem (3) for every $K \in \mathcal{A}_{m,n}$ i.e.

$$\min_{K \in \mathcal{A}_{m,n}} \left\{ \frac{1}{2} \int_D (u_K - f)^2 dx + \frac{\alpha}{2} \int_D |\nabla u_K - \nabla f|^2 dx \mid u_K \text{ solution of Problem 1.1} \right\}. \quad (7)$$

Here, we do not need to specified a size constraint on our admissible domains. Indeed, imposing $K \in \mathcal{A}_{m,n}$ implies a volume constraint and a geometrical constraint on K since K is formed by a finite number of balls with radius $mn^{-1/2}$. We set $v_K := u_K - f$. Then, v_K is in $H^1(D)$ and satisfies

Problem 3.1. Find v in $H^1(D)$ such that

$$\begin{cases} -\alpha \Delta v + v = g, & \text{in } D \setminus K, \\ v = 0, & \text{in } K, \\ \frac{\partial v}{\partial \mathbf{n}} = 0 & \text{on } \partial D, \end{cases} \quad (8)$$

where $g := -f + \alpha \Delta f$.

The optimization problem (7) can be reformulated as a compliance optimization problem

$$\min_{K \in \mathcal{A}_{m,n}} \left\{ \frac{1}{2} \int_D g v_K dx \mid v_K \text{ solution of Problem 3.1} \right\}. \quad (9)$$

We deal with Neumann boundary conditions on D . However, it is possible to cover the boundary with $\frac{2C_D}{m} n^{1/2}$ balls so that we have formally homogeneous Dirichlet boundary conditions on D . The well-posedness of such problem have been studied in the laplacian case in [32]. Without significant, change we have

Theorem 3.1. If D is an open bounded subset of \mathbb{R}^2 and if $g \geq 0$ is in $L^2(D)$, then problem (9) admit a unique solution.

If we denote by K_n^{opt} the solution, then we have that $\infty_{K_n^{\text{opt}}}$ γ -converge to ∞_D as n tends to $+\infty$. However, the numbers of pixels x_0 in D to keep goes also to infinity. Thus, it gives no relevant information on the distribution of the points to retain. As pointed out in [27], the local density of K_n^{opt} can be obtained by using a different topology for the Γ -convergence of the rescaled energies. In this new frame, the minimizers are unchanged but their behavior is seen from a different point of view. We define the probability measure μ_K for a given set K in $\mathcal{A}_{m,n}$ by

$$\mu_K := \frac{1}{n} \sum_{i=1}^n \delta_{x_i}.$$

We define the functional F_n from $\mathcal{P}(\bar{D})$ into $[0, +\infty]$ by

$$F_n(\mu) := \begin{cases} n \int_D g v_K dx & , \text{ if } \exists K \in \mathcal{A}_{m,n}, \text{ s.t. } \mu = \mu_K, \\ +\infty & , \text{ otherwise.} \end{cases}$$

The following Γ -convergence of F_n theorem is similar to the one given in Theorem 2.2. in [32].

Theorem 3.2. *If $g \geq 0$, then the sequence of functionals F_n , defined above, Γ -converge with respect to the weak \star topology in $\mathcal{P}(\bar{D})$ to*

$$F(\mu) := \int_D \frac{g^2}{\mu_a} \theta(m\mu_a^{1/2}) dx,$$

where $\mu = \mu_a dx + \nu$ is the Radon-Nikodym-Lebesgue decomposition of μ ([33], Theorem 3.8) with respect to the Lebesgue measure and

$$\theta(m) := \inf_{K_n \in \mathcal{A}_{m,n}} \liminf_{n \rightarrow +\infty} n \int_D g v_{K_n} dx,$$

where v_{K_n} solution of Problem 3.1.

As a consequence of the Γ -convergence stated in the theorem above, the empirical measure $\mu_{K_n^{\text{opt}}} \rightarrow \mu^{\text{opt}}$ weak \star in $\mathcal{P}(\mathbb{R}^d)$ where μ^{opt} is a minimizer of F . Unfortunately, the function θ is not known explicitly. We establish here after that θ is positive, non increasing and vanish after some point which will be enough for practical exploration. The next theorem gives an estimate of the function θ defined above. The proof is given in Appendix A.

Theorem 3.3. *We have, for m in $(0, t_1)$,*

$$C_1(\alpha) |\ln(m)| - C_2(\alpha) \leq \theta(m) \leq C_3(\alpha) |\ln(m)|,$$

where C_1, C_2 and C_3 are constants depending on α .

Remark. We can extend the results above to any g since we may formally split the discussion on the sets $\{g \geq 0\}$ and $\{g < 0\}$.

These estimates on θ suggest that to minimize F , when g^2 is large, μ_a should be large in order for θ to be close to its vanishing point, while when g^2 is small μ_a could be small. Formal Euler-Lagrange equation and the estimates on θ give the following information : to minimize

$$F(\mu) := \int_D \frac{g^2}{\mu_a} \theta(m\mu_a^{1/2}) dx,$$

one have to take

$$\frac{\mu_a^2}{|1 - \log \mu_a|} \approx c_{m,f} (f - \alpha \Delta f)^2.$$

This introduces a soft-thresholding with respect to the first approach. To sum up, we can choose the interpolation data such that the pixel density is increasing with $g^2 = (f - \alpha \Delta f)^2$. This soft-thresholding rule can be enforced with a standard digital halftoning. According to [17],[34] and [35], we recall that digital halftoning is a method of rendering that convert a continuous image to a binary image, for example black and white image, while giving the illusion of color continuity. This color continuity is simulated for the human eye by a spacial distribution of black and white pixels. Two different kinds of halftoning algorithms exist : dithering and error diffusion halftoning. The first one is based on a so-called dithering mask function, while the other one is an algorithm which propagate the error between the new value (0 or 1) and the old one (in the interval $[0, 1]$) [36]. An ideal digital halftoning method would conserves the average value of gray while giving the illusion of color continuity.

4 Time Dependent Compression Method

In this section, we propose an other method which depends on time.

Problem 4.1. For t in $(0, T]$, find $u(t, \cdot)$ in $H^1(D)$ such that

$$\begin{cases} \partial_t u(t, \cdot) - \alpha \Delta u(t, \cdot) = 0, & \text{in } D \setminus K_t, \\ u(t, \cdot) = f, & \text{in } K_t, \\ \frac{\partial u}{\partial \mathbf{n}}(t, \cdot) = 0, & \text{on } \partial D, \end{cases} \quad (10)$$

and

$$\begin{cases} u(0, \cdot) \in L^2(D), \\ K_0 \subset D. \end{cases}$$

Using implicit scheme in time,

Problem 4.2. For $n \in \mathbb{N}$, by knowing u^n , find u^{n+1} in $H^1(D)$ such that

$$\begin{cases} u^{n+1} - \delta t \alpha \Delta u^{n+1} = u^n, & \text{in } D \setminus K_n, \\ u^{n+1} = f, & \text{in } K_n, \\ \frac{\partial u^{n+1}}{\partial \mathbf{n}} = 0, & \text{on } \partial D, \end{cases} \quad (11)$$

and

$$\begin{cases} u^0 \in L^2(D), \\ K_0 \subset D. \end{cases}$$

The associated energy is

$$J(u^{n+1}) := \frac{1}{2} \int_D |u^{n+1}|^2 dx + \frac{\delta t \alpha}{2} \int_D |\nabla u^{n+1}|^2 dx - \int_D u^n u^{n+1} dx.$$

Problem 4.2 is very close to Problem 1.1. The differences are that we have a second member u^n and that the known mask, namely K_n , depends on n . Since the inpainting mask in our model is time-dependent, we propose, in Section 5, various methods to construct K_n for $n > 0$.

4.1 Problem Reformulation

Now, we want to give a max-min formulation, similar to Proposition 1.1, of the optimization problem (3) with Problem 4.2.

Proposition 4.1. Our optimization problem (3) can be rewritten

$$\max_{K^n} \min_{u^{n+1}} \frac{1}{2} \int_D |u^{n+1}|^2 + \frac{\delta t \alpha}{2} \int_D |\nabla u^{n+1}|^2 - \int_D u^n u^{n+1}.$$

4.2 Topological Gradient

Like for Section 2, we use a topological gradient based algorithm to compute the solution of our optimization problem. Again, let us define K_ε the compact set $K \setminus B(x_0, \varepsilon)$ where $B(x_0, \varepsilon)$ is the ball centered in $x_0 \in D$ with radius $\varepsilon > 0$ such that $B(x_0, \varepsilon) \subset K$. Let us denote by j the functional, for u^n in $H^1(D)$ given,

$$j : A \in \mathcal{P}(D) \mapsto \min_{u \in H^1(D), u=f \text{ in } A} \frac{\delta t \alpha}{2} \int_D |\nabla u|^2 dx + \frac{1}{2} \int_D u^2 dx - \int_D u^n u dx.$$

Finally, we denote by u_ε the minimizer of $j(K_\varepsilon)$. Then, we have

Theorem 4.1. *With notations from above, we have when ε tends to 0,*

$$j(K_\varepsilon) - j(K) = (f(x_0) - \delta t \alpha \Delta f(x_0) - u(x_0))^2 \pi \varepsilon^4 \ln(\varepsilon) + O(\varepsilon^4).$$

Proof. For simplicity, we write u_ε instead of u_ε^{n+1} and u instead of u^n . Thus, we have

$$\begin{aligned} j(K_\varepsilon) - j(K) &= \frac{\delta t \alpha}{2} \int_{B(x_0, \varepsilon)} |\nabla u_\varepsilon|^2 dx + \frac{1}{2} \int_{B(x_0, \varepsilon)} u_\varepsilon^2 dx - \int_{B(x_0, \varepsilon)} u u_\varepsilon dx \\ &\quad - \frac{\delta t \alpha}{2} \int_{B(x_0, \varepsilon)} |\nabla f|^2 dx - \frac{1}{2} \int_{B(x_0, \varepsilon)} f^2 dx + \int_{B(x_0, \varepsilon)} u f dx. \end{aligned}$$

The variational formulation gives us

$$\int_{B(x_0, \varepsilon)} u_\varepsilon^2 dx + \delta t \alpha \int_{B(x_0, \varepsilon)} |\nabla u_\varepsilon|^2 dx = \int_{B(x_0, \varepsilon)} u_\varepsilon f dx + \delta t \alpha \int_{B(x_0, \varepsilon)} \nabla u_\varepsilon \cdot \nabla f dx + \int_{B(x_0, \varepsilon)} u(u_\varepsilon - f) dx.$$

Then,

$$\begin{aligned} j(K_\varepsilon) - j(K) &= \frac{1}{2} \int_{B(x_0, \varepsilon)} u_\varepsilon f dx + \frac{\delta t \alpha}{2} \int_{B(x_0, \varepsilon)} \nabla u_\varepsilon \cdot \nabla f dx - \frac{1}{2} \int_{B(x_0, \varepsilon)} u(u_\varepsilon - f) dx \\ &\quad - \frac{\delta t \alpha}{2} \int_{B(x_0, \varepsilon)} |\nabla f|^2 dx - \frac{1}{2} \int_{B(x_0, \varepsilon)} f^2 dx \\ &= \frac{1}{2} \int_{B(x_0, \varepsilon)} f(u_\varepsilon - f) dx + \frac{\delta t \alpha}{2} \int_{B(x_0, \varepsilon)} \nabla f \cdot \nabla (u_\varepsilon - f) dx - \frac{1}{2} \int_{B(x_0, \varepsilon)} u(u_\varepsilon - f) dx \\ &= \frac{1}{2} \int_{B(x_0, \varepsilon)} f(u_\varepsilon - f) dx - \frac{\delta t \alpha}{2} \int_{B(x_0, \varepsilon)} \Delta f (u_\varepsilon - f) dx - \frac{1}{2} \int_{B(x_0, \varepsilon)} u(u_\varepsilon - f) dx \\ &= \frac{1}{2} \int_{B(x_0, \varepsilon)} (f - \delta t \alpha \Delta f - u)(u_\varepsilon - f) dx. \end{aligned}$$

We have $(f - \delta t \alpha \Delta f - u) = (f - \delta t \alpha \Delta f - u)(x_0) + \|x - x_0\|O(1)$, and hence

$$j(K_\varepsilon) - j(K) = \frac{1}{2} (f(x_0) - \delta t \alpha \Delta f(x_0) - u(x_0)) \int_{B(x_0, \varepsilon)} (u_\varepsilon - f) dx + O(\varepsilon) \int_{B(x_0, \varepsilon)} (u_\varepsilon - f) dx.$$

Ones again, it is enough to compute the fundamental term in the asymptotic development of the expression $\int_{B(x_0, \varepsilon)} u_\varepsilon - f dx$. This is done by using Proposition B.1 with, $w = u_\varepsilon - f$ and $g = -f + \delta t \alpha \Delta f + u$. \square

This result conclude the theoretical part of this paper. In the remaining part, we confront our results to real cases.

5 Numerical Results

In this last section, we present some numerical results. We begin by comparing different masks to confirm our work from Section 2 and Section 3. Then, we present four time-dependent methods, that use results from Section 4, and compare them. Finally, we propose two different ways to deal with colored images. We use finite differences to compute approximated solutions of involved problems.

5.1 Masks Comparison

We compare the L^2 -error of the interpolation for different masks using Problem 1.1. For these experiments, we use the well-known grayscale image called ‘‘Lena’’, which size is 256×256 pixels, Figure 2 (a). We apply gaussian noise of different deviation, denoted by σ , and we compare the following masks : ‘‘Optimized’’ corresponds to the mask derived

from the topological gradient in Section 2, “Halfoned Optimized” corresponds to the mask derived from Section 3, “H1” correspond to the mask found in [17], “Halfoned H1” correspond to the halfoned mask found in [17], “Random” is a mask where pixels are selected randomly and “B-Tree” is the mask described in [19]. We denote by f the original image, by f_n the noised image, by u the reconstructed image, by “Norm” the error $\|f_n - u\|_{L^2(D)}$ and by $\#K$ the number of pixels saved in the inpainting mask K . Figure 2 and Figure 3 are reconstructions for $\alpha = 3$, with and without noise respectively.

σ	Optimized		Halfoned Optimized		H1		Halfoned H1		Random		B-Tree	
	Norm	$\#K$	Norm	$\#K$	Norm	$\#K$	Norm	$\#K$	Norm	$\#K$	Norm	$\#K$
0.00	100.13	6553	51.66	6488	117.80	6553	93.80	6492	74.58	6624	56.91	6597
0.05	73.24	6553	47.63	6494	76.05	6553	60.26	6508	69.49	6615	55.69	6528
0.10	67.61	6553	51.08	6492	76.14	6553	63.40	6504	72.78	6560	62.24	6510

Table 1: L^2 -error comparison for different masks by taking 10% of pixels, and applying Problem 1.1 with $\alpha = 3$.



(a) Original image.



(b) Optimized mask.

(c) Reconstruction with the optimized mask. $\|f - u\|_{L^2(D)} = 100.13$, $\#K = 6553$.

(d) Halftoned optimized mask.

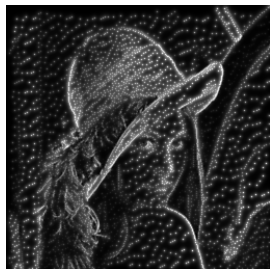
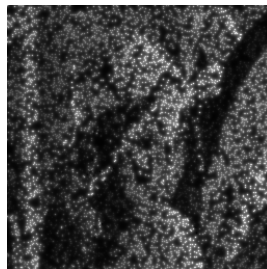
(e) Reconstruction with the halftoned optimized mask. $\|f - u\|_{L^2(D)} = 51.66$, $\#K = 6488$.(f) Reconstruction with the "H1" mask. $\|f - u\|_{L^2(D)} = 117.80$, $\#K = 6553$.(g) Reconstruction with the "Halftoned H1" mask. $\|f - u\|_{L^2(D)} = 93.80$, $\#K = 6492$.(h) Reconstruction with the random mask. $\|f - u\|_{L^2(D)} = 74.58$, $\#K = 6624$.(i) Reconstruction with the B-Tree mask. $\|f - u\|_{L^2(D)} = 56.91$, $\#K = 6597$.

Figure 2: Masks comparison for Problem 1.1 by saving 10% of pixels.

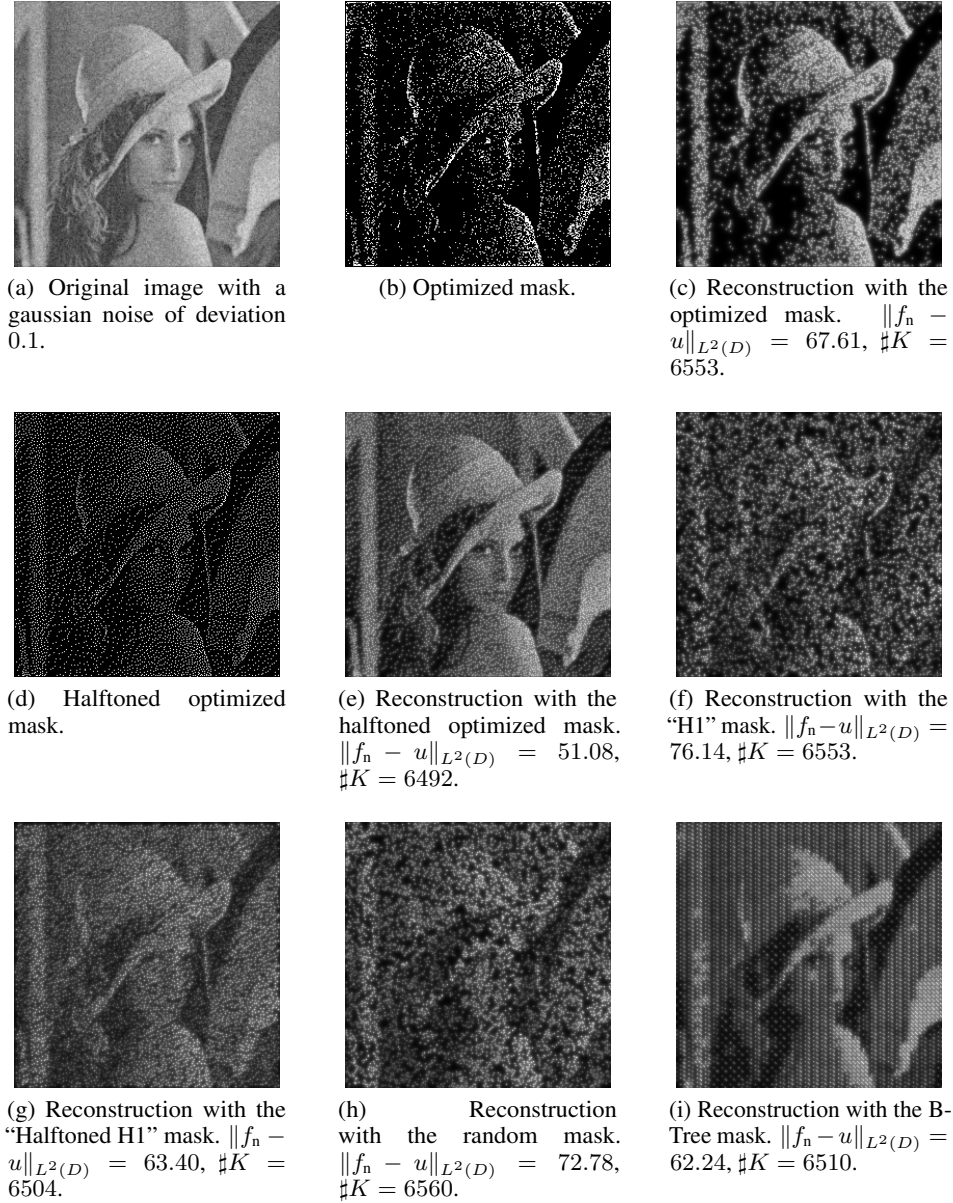


Figure 3: Masks comparison with gaussian noise for Problem 1.1 by saving 10% of pixels.

As expected from our mathematical analysis, masks "Optimized" and "Halftoned Optimized" globally gives the lowest L^2 -error for Problem 1.1 and the best visual results. The two "H1" masks are not efficient coupled with Problem 1.1 since they have been designed for the Homogeneous Diffusion inpainting (i.e. for $\alpha \rightarrow +\infty$). Moreover, since these masks only depends on $|\Delta f|^2$, they are very sensitive to gaussian noise. The B-Tree algorithm, by its nature, induce visible artifacts, which leads to this mosaic visual.

5.2 Methods Comparison

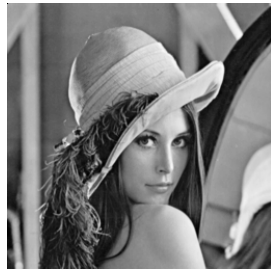
Now, we propose different methods to construct mask and reconstruct image and compare them to the method described in [17], denoted "H1" in the sequel, i.e. the "H1" mask coupled with homogeneous diffusion inpainting. The method denoted by "L2" is the one with the halftoned mask from Section 3 along with Problem 1.1. The remaining methods use the parabolic Problem 4.2 as follow :

- Encoding : For the “L2Sta” method, we use the same mask, for all n in $\{0, \dots, N\}$, as for the “L2” method, i.e. the halftoned mask from Section 3. For the “L2Dec” method, the “L2Inc” method and the “L2Insta” method, we use algorithms described in Appendix C.
- Decoding : For each methods, we use only the last K_n from the encoding step and inpaint with Problem 4.2 until a fixed time.

σ	H1		L2		L2Sta		L2Dec		L2Inc		L2Insta	
	Norm	#K	Norm	#K	Norm	#K	Norm	#K	Norm	#K	Norm	#K
0.00	11.95	6492	47.91	6486	24.50	6488	31.61	6553	12.99	6520	9.63	6514
0.10	14.04	6503	46.06	6492	16.39	6484	14.61	6553	10.52	6520	13.19	6491

Table 2: L^2 -error comparison for different masks by taking 10% of pixels for the following methods : “L2” with $\alpha = 3.61$, “L2Sta” with $\alpha = 10$, “L2Dec” with $\alpha = 30$, $N = 35$, “L2Inc” with $\alpha = 8$, $N = 40$ and “L2Insta” with $\alpha = 10$, $N = 10$.

Figure 4 and Figure 5 are examples of reconstructed image with methods described before, without noise and with a gaussian noise of deviation $\sigma = 0.1$ respectively.



(a) Original image.

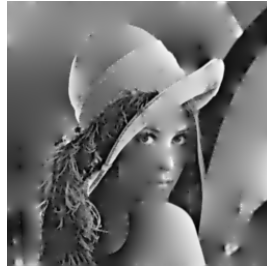
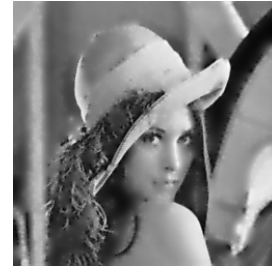
(b) Reconstruction using method "H1".
 $\|u - f\|_{L^2(D)} = 11.95$,
 $\#K = 6492$.(c) Reconstruction using method "L2".
 $\|u - f\|_{L^2(D)} = 47.91$,
 $\#K = 6486$.(d) Reconstruction using method "L2Sta".
 $\|u - f\|_{L^2(D)} = 24.50$,
 $\#K = 6488$.(e) Reconstruction using method "L2Dec".
 $\|u - f\|_{L^2(D)} = 31.61$,
 $\#K = 6553$.(f) Reconstruction using method "L2Inc".
 $\|u - f\|_{L^2(D)} = 12.99$,
 $\#K = 6520$.(g) Reconstruction using method "L2Insta".
 $\|u - f\|_{L^2(D)} = 9.63$,
 $\#K = 6514$.

Figure 4: Image reconstruction using various methods, with 10% of total pixels saved. "L2" with $\alpha = 3.61$, "L2Sta" with $\alpha = 10$, "L2Dec" with $\alpha = 30$, $N = 35$, "L2Inc" with $\alpha = 8$, $N = 40$ and "L2Insta" with $\alpha = 10$, $N = 10$.



(a) Original image with a gaussian noise of deviation 0.1.



(b) Reconstruction using method "H1".
 $\|u - f_n\|_{L^2(D)} = 14.04$,
 $\#K = 6503$.



(c) Reconstruction using method "L2".
 $\|u - f_n\|_{L^2(D)} = 46.06$,
 $\#K = 6492$.



(d) Reconstruction using method "L2Sta".
 $\|u - f_n\|_{L^2(D)} = 16.39$,
 $\#K = 6484$.



(e) Reconstruction using method "L2Dec".
 $\|u - f_n\|_{L^2(D)} = 14.61$,
 $\#K = 6553$.



(f) Reconstruction using method "L2Inc".
 $\|u - f_n\|_{L^2(D)} = 10.52$,
 $\#K = 6520$.



(g) Reconstruction using method "L2Insta".
 $\|u - f_n\|_{L^2(D)} = 13.19$,
 $\#K = 6491$.

Figure 5: Image reconstruction using various methods, with 10% of total pixels saved and a gaussian noise of deviation $\sigma = 0.1$ applied to the input image.

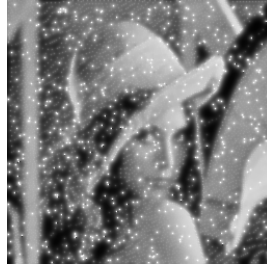
The "H1" method seems to give a nice visual quality on Figure 4 (b). However, since its mask only depends on $|\Delta f|^2$, it is very sensitive to gaussian noise. That is why, when applying gaussian noise to the input image, Figure 5 (b), the quality decrease quickly. It is interesting to remark that, without noise, the "L2Insta" method gives lower L^2 -error than the "H1" one. The "L2" method (c) and the "L2Sta", use the same mask. However, in the "L2Sta" case, we use the time-dependent inpainting which leads to a more pleasant visual result. Indeed, the time-dependent inpainting allows a biggest diffusion of mask's pixels and, as a result, fills the black gap between mask's pixels. The "L2Inc" method gives also great results. It might be due to the fact that for each iteration, we add to the mask a small amount of best pixels for the current iteration. Thus, we keep important pixels for previous iterations. Contrasting with the "L2Inc" method, the "L2Dec" method remove, for each iteration, a small amount of inadequate pixels for the current iteration. Thus it is possible to remove important pixels for previous iterations. It is the same for the "L2Insta" method, but it is possible to remove all significant pixels for previous iterations. To conclude, our proposed methods seems to be more robust to gaussian noise than methods proposed in the literature.

5.3 Salt and Pepper Noise

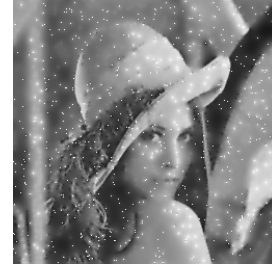
Now, we confront our methods to salt and pepper noise. Figure 6 are experiments with 1% of salt noise for the first row, and with 1% of pepper noise for the second one.



(a) Original image with 1% of salt noise.



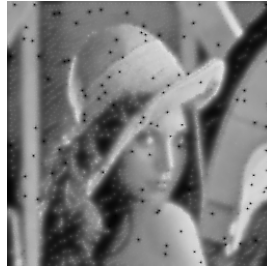
(b) Reconstruction using method "L2Sta".
 $\|u - f_n\|_{L^2(D)} = 25.33$,
 $\#K = 6477$.



(c) Reconstruction using method "L2Inc".
 $\|u - f_n\|_{L^2(D)} = 12.17$,
 $\#K = 6520$.



(d) Original image with 1% of pepper noise.



(e) Reconstruction using method "L2Sta".
 $\|u - f_n\|_{L^2(D)} = 22.78$,
 $\#K = 6479$.



(f) Reconstruction using method "L2Inc".
 $\|u - f_n\|_{L^2(D)} = 11.5$,
 $\#K = 6520$.

Figure 6: Image reconstruction using proposed methods, with 10% of total pixels saved and 1% of salt noise applied to the input image.

Our experiments show that our methods do not give satisfying reconstruction when the input image is significantly corrupted by salt and pepper noise. The diffusion inpainting amplifies the noise by making stains due to noise bigger. This is expected since our method is design to minimize the L^2 -error which is not suited to remove impulse noise like salt and pepper noise. We suggest to minimize the L^1 -error instead [37, 38].

5.4 Colored Images

Finally, we propose two strategies for creating masks for colored images. A colored images can be modeled by a function f from D to $[0, 1]^3$, $x \mapsto (f_R(x), f_G(x), f_B(x))^T$, where functions f_R , f_G and f_B are from D to \mathbb{R} , represent red channel, green channel and blue channel respectively. The first strategy consists in creating three masks, one for each channel. This is done in Figure 7 where (a) is the original image, (b) is the mask by keeping 10% of total pixels for each masks and (c) is the reconstructed image. The second strategy is to convert the image into grayscale image, create a mask for the grayscale image and to use it for each channel. This strategy have been applied to Figure 7 (d), (e), by keeping 10% of total pixels, (f), (g), by keeping 15% of total pixels and (h), (i), by keeping 20% of total pixels. In these experiments we used method "L2Inc" with $\alpha = 8$ and $N = 40$.

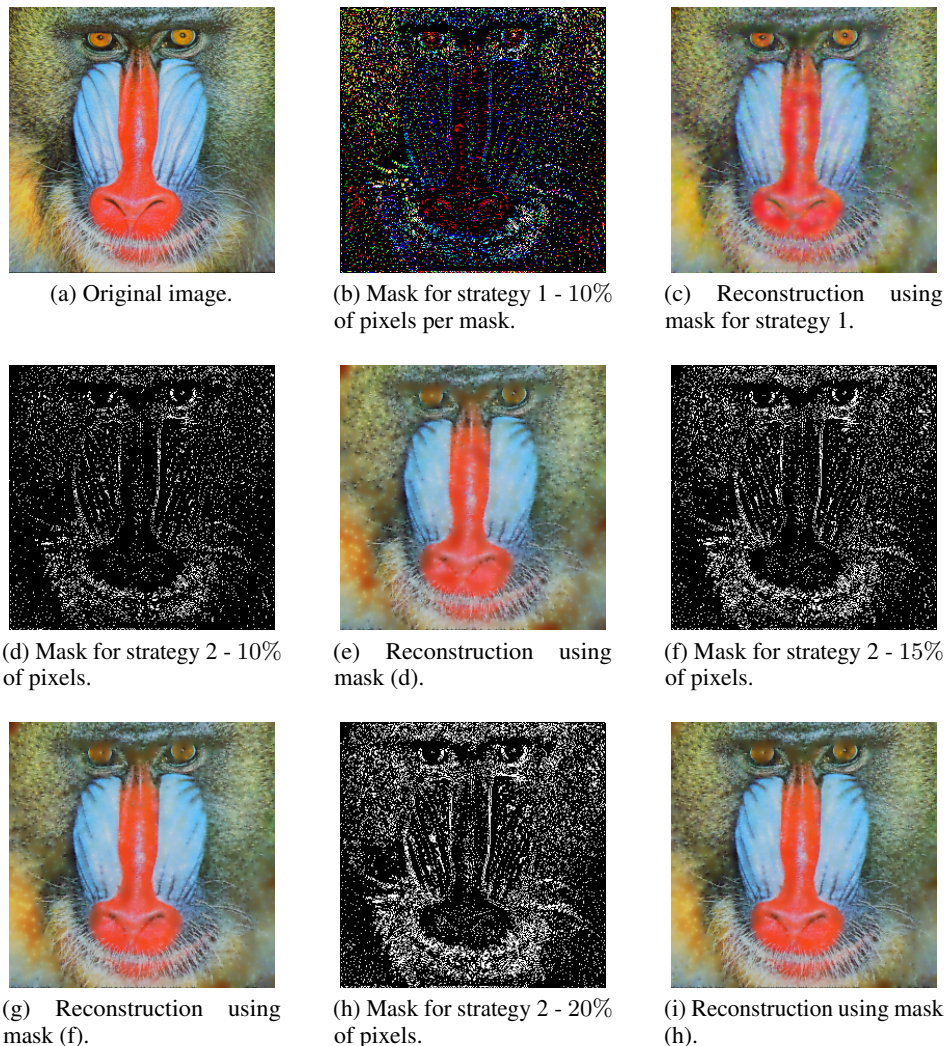


Figure 7: Masks and reconstructions for colored images using “L2Inc” method with $\alpha = 8$ and $N = 40$.

Since in strategy 1 we compute mask with a fixed amount of pixels for each channel, the final mask, where the three masks are combined, may not have the same number of pixels. Indeed, the three masks may not have common pixels or only some common pixels. As expected, strategy 1 gives lower L^2 -error than strategy 2. It can be notice easily be looking at the eyes of the monkey : For strategy 1 they are well-reconstructed but for strategy 2, even with 20% of saved pixels, the reconstruction is not satisfying. An other tempting idea would be to save one mask per color channel, like strategy 1, but with a different amount of pixels for each channel. Indeed, due to color wavelength, the gaussian noise sensitivity is different for channels : the one with large wavelength are less sensitive than the one with thin wavelength.

Summary and Conclusions

We introduced a mathematical model of the compression problem and its relaxed formulation in the framework of Γ -convergence. To construct an inpainting mask, we investigated two shape optimization approaches. We obtained a criterion to create a optimal set by using thresholding. The second approach consists in considering “fat pixels” instead of a set of single isolated pixel it yields to a softing of the criteria. We extended our methods to time-dependent problems which result in two-fold improvement of the stationary approach : First, smoothing hard thresholding in the selection for the coding step and giving away to build adaptively the final mask. Secondly, in the decoding phase, it performs the denoising of the input image. We introduced and implemented several algorithms to obtain an optimal mask and, for reconstruction phase, this induces a higher visual result than the stationary method. Numerical experiments confirm that our methods are highly efficient when images are corrupted by gaussian noise. Furthermore, they suggest to favor

the density models for the stationary problem and the increasing mask strategy, that we called “L2Inc”, for the time dependent problems. We confront our methods to salt and pepper, but they do not give satisfying reconstruction when the input image is significantly corrupted by such noise. This was expected since minimizing the L^2 -error is not the best way to remove impulse noise like salt and pepper noise. We extended the numerical experiments to color images following two procedures. The first one consists in creating three masks, one for each channel, while the second creates a mask for the grayscale image and use this mask for each channel. The first approach gives better reconstruction.

References

- [1] Yehuda Dar, Michael Elad, and Alfred Bruckstein. System-aware compression. 01 2018.
- [2] Majid Rabbani and Paul W. Jones. *Digital Image Compression Techniques*. Society of Photo-Optical Instrumentation Engineers (SPIE), USA, 1st edition, 1991.
- [3] David Taubman and Michael Marcellin. *JPEG2000 Image Compression Fundamentals, Standards and Practice*. Springer Publishing Company, Incorporated, 2013.
- [4] Macarena Boix and Begoña Cantó. Wavelet transform application to the compression of images. *Mathematical and Computer Modelling*, 52(7):1265 – 1270, 2010. Mathematical Models in Medicine, Business & Engineering 2009.
- [5] Tony F. Chan and Hao-Min Zhou. Total variation wavelet thresholding. *Journal of Scientific Computing*, 32(2):315–341, Aug 2007.
- [6] David Tschumperlé and Rachid Deriche. Vector-Valued Image Regularization with PDE’s : A Common Framework for Different Applications. *IEEE Transactions on Pattern Analysis and Machine Intelligence*, 27(4):506–517, 2005.
- [7] S. Masnou and J. . Morel. Level lines based disocclusion. In *Proceedings 1998 International Conference on Image Processing. ICIP98 (Cat. No.98CB36269)*, pages 259–263 vol.3, 1998.
- [8] D. Rotem and Y. Zeevi. Image reconstruction from zero crossings. *IEEE Transactions on Acoustics, Speech, and Signal Processing*, 34(5):1269–1277, 1986.
- [9] Irena Galić, Joachim Weickert, Martin Welk, Andrés Bruhn, Alexander Belyaev, and Hans-Peter Seidel. Towards pde-based image compression. In Nikos Paragios, Olivier Faugeras, Tony Chan, and Christoph Schnörr, editors, *Variational, Geometric, and Level Set Methods in Computer Vision*, pages 37–48, Berlin, Heidelberg, 2005. Springer Berlin Heidelberg.
- [10] Marcelo Bertalmio, Guillermo Sapiro, Vincent Caselles, and Coloma Ballester. Image inpainting. In *Proceedings of the 27th Annual Conference on Computer Graphics and Interactive Techniques, SIGGRAPH ’00*, page 417–424, USA, 2000. ACM Press/Addison-Wesley Publishing Co.
- [11] Folkmar Bornemann and Tom März. Fast image inpainting based on coherence transport. *Journal of Mathematical Imaging and Vision*, 28:259–278, 10 2007.
- [12] Tony Chan and Jackie Shen. Nontexture inpainting by curvature-driven diffusions. *Journal of Visual Communication and Image Representation*, 12:436–449, 12 2001.
- [13] Joachim Weickert, Wissenschaftlicher Werdegang, Steven Zucker, Allan Dobbins, Lee Iverson, B. Kimia, and Allen Tannenbaum. Anisotropic diffusion in image processing, 01 1996.
- [14] Theljani Anis. *Partial differential equations methods and regularization techniques for image inpainting*. PhD thesis, University of Tunis El Manar and University of Haute-Alsace, 11 2015.
- [15] Harald Köstler, Markus Stürmer, C Freundl, and Ulrich Rüdè. Pde based video compression in real time. 08 2007.
- [16] D. Liu, X. Sun, F. Wu, S. Li, and Y. Zhang. Image compression with edge-based inpainting. *IEEE Transactions on Circuits and Systems for Video Technology*, 17(10):1273–1287, Oct 2007.
- [17] Zakaria Belhachmi, Dorin Bucur, Bernhard Burgeth, and Joachim Weickert. How to choose interpolation data in images. *SIAM Journal of Applied Mathematics*, 70:333–352, 01 2009.
- [18] Holger Dell. Seed points in pde-driven interpolation, Jun 2006.
- [19] Riccardo Distasi, Michele Nappi, and Sergio Vitulano. Image compression by b-tree triangular coding. 45:1095–1100, 1997.
- [20] Christian Schmaltz, Pascal Peter, Markus Mainberger, Franziska Ebel, Joachim Weickert, and Andrés Bruhn. Understanding, optimising, and extending data compression with anisotropic diffusion. *International Journal of Computer Vision*, 108(3):222–240, Jul 2014.

- [21] Laurent Hoeltgen, Markus Mainberger, Sebastian Hoffmann, Joachim Weickert, Ching Hoo Tang, Simon Setzer, Daniel Johannsen, Frank Neumann, and Benjamin Doerr. Optimising spatial and tonal data for pde-based inpainting. *CoRR*, abs/1506.04566, 2015.
- [22] E. J. Candes, J. Romberg, and T. Tao. Robust uncertainty principles: exact signal reconstruction from highly incomplete frequency information. *IEEE Transactions on Information Theory*, 52(2):489–509, Feb 2006.
- [23] G. Wetzstein. Ee 367 / cs 448 i computational imaging and display notes : Noise , denoising , and image reconstruction with noise (lecture 10). 2017.
- [24] S. V. Venkatakrisnan, C. A. Bouman, and B. Wohlberg. Plug-and-play priors for model based reconstruction. In *2013 IEEE Global Conference on Signal and Information Processing*, pages 945–948, 2013.
- [25] A. N. Tikhonov and Vasiliy Yakovlevich Arsenin. Solutions of ill-posed problems. 1977.
- [26] Gianni Dal Maso. *An Introduction to Γ -Convergence*, volume 8 of *Progress in Nonlinear Differential Equations and Their Applications*. Birkhäuser Basel, 1993.
- [27] Dorin Bucur and Giuseppe Buttazzo. Variational methods in shape optimization problems. *Progress in Nonlinear Differential Equations and Their Application*, 01 2005.
- [28] Gianni Dal Maso. γ -convergence and μ -capacities. *Annali della Scuola Normale Superiore di Pisa - Classe di Scienze*, Ser. 4, 14(3):423–464, 1987.
- [29] Gianni Dal Maso and François Murat. Asymptotic behaviour and correctors for dirichlet problems in perforated domains with homogeneous monotone operators. *Annali della Scuola Normale Superiore di Pisa - Classe di Scienze*, Ser. 4, 24(2):239–290, 1997.
- [30] Stanislas Larnier, Jérôme Fehrenbach, and Mohamed Masmoudi. The topological gradient method: From optimal design to image processing. *Milan Journal of Mathematics*, 80(2):411–441, Dec 2012.
- [31] Stéphane Garreau, Philippe Guillaume, and Mohamed Masmoudi. The topological asymptotic for pde systems: The elasticity case. *SIAM Journal on Control and Optimization*, 39(6):1756–1778, 2001.
- [32] Giuseppe Buttazzo, Filippo Santambrogio, and Nicolas Varchon. Asymptotics of an optimal compliance-location problem. *ESAIM: Control, Optimisation and Calculus of Variations*, 12, 04 2005.
- [33] Gerald B. Folland. *Real Analysis: Modern Techniques and Their Applications, 2nd Edition*. Pure and Applied Mathematics: A Wiley Series of Texts, Monographs and Tracts. Wiley-Blackwell, 1999.
- [34] Robert Ulichney. *Digital Halftoning*. MIT Press, Cambridge, MA, USA, 1987.
- [35] Roy L. Adler, Bruce Kitchens, Marco Martens, Charles Philippe Tresser, and Chai Wah Wu. The mathematics of halftoning. *IBM Journal of Research and Development*, 47:5–16, 2003.
- [36] R. Floyd and L. S. Steinberg. An adaptive algorithm for spatial gray scale. 1975.
- [37] Mila Nikolova. Minimizers of cost-functions involving nonsmooth data-fidelity terms. application to the processing of outliers. *SIAM J. Numerical Analysis*, 40:965–994, 09 2002.
- [38] Mila Nikolova. A variational approach to remove outliers and impulse noise. *Journal of Mathematical Imaging and Vision*, 20, 01 2004.
- [39] Lawrence C. Evans. *Partial differential equations*. American Mathematical Society, Providence, R.I., 2010.
- [40] L. E. Payne and H. F. Weinberger. An optimal poincaré inequality for convex domains. *Archive for Rational Mechanics and Analysis*, 5(1):286–292, Jan 1960.
- [41] Keith B. Oldham, Jan Myland, and Jerome Spanier. *An Atlas of Functions, with Equator, the Atlas Function Calculator*. Springer-Verlag New York, 2009.
- [42] D.G. Duffy. *Green’s functions with applications, second edition*. 01 2015.

A Proof of the Estimate of θ

We aim to give some estimate of the function θ defined in Theorem 3.2. In the sequel, we set $t_1 := \frac{\sqrt{2}}{2}$. We will widely use the following maximum principle of Problem 3.1 for the proofs.

Theorem A.1 (Weak maximum principle). *Let us assume that the solution of Problem 3.1 v_K is in $C^2(D) \cap C^0(\bar{D})$. If $g \geq 0$ in $D \setminus K$, then $v_K \geq 0$ in D .*

Proof. See [39] Theorem 2 in Section 6.4. □

Moreover, we will need the following properties :

Lemma A.1. *If v_K is the solution of Problem 3.1, then v_K satisfies*

$$\|v_K\|_{L^2(D)} \leq (1 + \alpha C(D))^{-1} \|g\|_{L^2(D)}$$

and

$$\|v_K\|_{L^1(D)} \leq |D|^{1/2} (1 + \alpha C(D))^{-1} \|g\|_{L^2(D)}.$$

Proof. Using the weak formulation and Poincaré inequality, we get

$$\|v_K\|_{L^2(D)}^2 = \int_D v_K^2 dx = \int_D g v_K dx - \alpha \int_D |\nabla v_K|^2 dx \leq \int_D g v_K dx - \alpha C(D) \int_D v_K^2 dx.$$

Hölder inequality gives us

$$\|v_K\|_{L^2(D)}^2 \leq \|g\|_{L^2(D)} \|v_K\|_{L^2(D)} - \alpha C(D) \|v_K\|_{L^2(D)}^2.$$

$$\|v_K\|_{L^2(D)} \leq \|g\|_{L^2(D)} - \alpha C(D) \|v_K\|_{L^2(D)} \Leftrightarrow \|v_K\|_{L^2(D)} \leq (1 + \alpha C(D))^{-1} \|g\|_{L^2(D)}$$

Again, using Hölder inequality

$$\|v_K\|_{L^1(D)} \leq |D|^{1/2} \|v_K\|_{L^2(D)} \leq |D|^{1/2} (1 + \alpha C(D))^{-1} \|g\|_{L^2(D)}.$$

□

Remark. If $D \subset \mathbb{R}^2$ is convex we have, according to [40],

$$\|v_K\|_{L^2(D)} \leq (1 + \alpha \pi^2 \text{diam}(D)^{-2})^{-1} \|g\|_{L^2(D)}.$$

$$\|v_K\|_{L^1(D)} \leq |D|^{1/2} (1 + \alpha \pi^2 \text{diam}(D)^{-2})^{-1} \|g\|_{L^2(D)}.$$

Moreover, if $g = 1$, we have $\|v_K\|_{L^1(D)} \leq (1 + \alpha \pi^2 \text{diam}(D)^{-2})^{-1} |D|$.

Lemma A.2. *We have, for m in $(0, t_1)$,*

$$\theta(m) \leq C_1(\alpha) \ln m^{-1} + C_2(\alpha),$$

where C_1 and C_2 are constants depending on α .

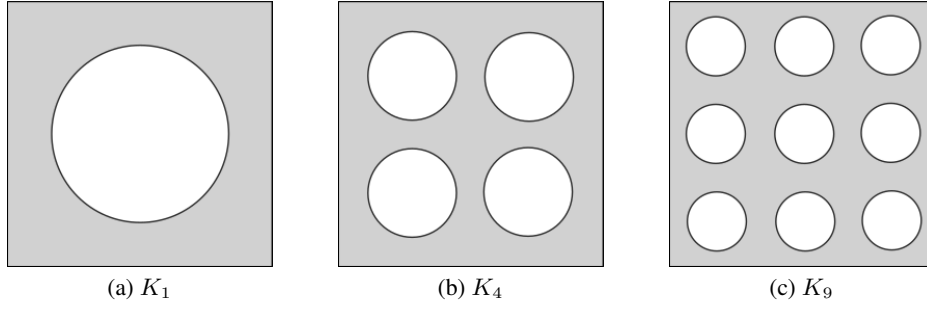


Figure 8: Drawing of $I^2 \setminus K_n$ with $n := k^2$, for $k = 1, 2, 3$.

Proof. We consider a particular family of sets K_n in $\mathcal{A}_{m,n}$. We choose an integer k such that $n = k^2$ and we suppose $K_n \in \mathcal{A}_{m,n}$ are composed of n balls of radius m/k , with their centers superposing the centers of the k^2 squares of side $1/k$ of a regular lattice partitioning the square I^2 .

Let us denote $v_{K_n}^1$ the solution of Problem 3.1 with $g = 1$, $K = K_n$ and $D = I^2$. It holds $\int_I v_{K_n}^1 dx = n \int_I v_{K_1}^1 dx$. We recall

$$\theta(m) := \inf_{K_n \in \mathcal{A}_{m,n}} \liminf_n n \int_D g v_{K_n} dx.$$

In particular

$$\theta(m) \leq \liminf_n n \int_D v_{K_n}^1 dx = \int_I v_{K_1}^1 dx.$$

We have $I^2 \subset B(x_0, t_1)$. Therefore if we denote by w the solution of Problem 3.1 with $g = 1$, $D = B(x_0, t_1)$ and $K = K_1 := B(x_0, m)$, it holds by the maximum principle that $v_{K_1}^1 \leq w$. Then we have the following estimate

$$\theta(m) \leq \int_{B(x_0, t_1)} w dx.$$

Let us consider the following problem

$$\begin{cases} -\alpha \Delta \tilde{w} = 1 & \text{in } B(x_0, t_1) \setminus \overline{B(x_0, m)}, \\ \tilde{w} = 0 & \text{in } B(x_0, m), \\ \frac{\partial \tilde{w}}{\partial \mathbf{n}} = 0 & \text{on } \partial B(x_0, t_1). \end{cases} \quad (12)$$

Now, we set $e := w - \tilde{w}$. Thus we have for all v in $H_0^1(B(x_0, t_1) \setminus \overline{B(x_0, m)})$

$$\alpha \int_B \nabla e \cdot \nabla v dx = \alpha \int_B \nabla w \cdot \nabla v dx - \alpha \int_B \nabla \tilde{w} \cdot \nabla v dx = - \int_B w v dx,$$

i.e. e satisfies the problem below

$$\begin{cases} -\alpha \Delta e = -w & \text{in } B(x_0, t_1) \setminus \overline{B(x_0, m)}, \\ e = 0 & \text{in } B(x_0, m), \\ \frac{\partial e}{\partial \mathbf{n}} = 0 & \text{on } \partial B(x_0, t_1). \end{cases} \quad (13)$$

Since $w \geq 0$, we have by the maximum principle that $e \leq 0$ i.e. $0 \leq w \leq \tilde{w}$. By consequence

$$\theta(m) \leq \int_{B(x_0, t_1)} \tilde{w} dx.$$

The solution \tilde{w} have been computed in [32]. Due to the radial symmetry of \tilde{w} , we can get explicitly \tilde{w} , solution of :

$$\begin{cases} \tilde{w}''(r) + \frac{1}{r}\tilde{w}'(r) = -\frac{1}{\alpha} & \text{if } m < r < t_1, \\ \tilde{w} = 0 & \text{if } 0 \leq r \leq m, \\ \tilde{w}'(t_1) = 0 & . \end{cases} \quad (14)$$

For $r = |x - x_0|$ we have

$$\tilde{w}(x) = \begin{cases} k \ln\left(\frac{r}{m}\right) - \frac{1}{4\alpha}(r^2 - m^2) & \text{if } m < r < t_1, \\ 0 & \text{if } 0 \leq r \leq m \end{cases}, \quad k = \frac{mt_1^2}{2\alpha}.$$

Integrating \tilde{w} over $B(x_0, t_1)$

$$\begin{aligned} \int_{B(x_0, t_1)} \tilde{w} \, dx &= 2\pi \int_m^{t_1} \left(k \ln\left(\frac{r}{m}\right) - \frac{1}{4\alpha}(r^2 - m^2) \right) r \, dr \\ &= 2\pi k \int_m^{t_1} r \ln\left(\frac{r}{m}\right) \, dr - \frac{\pi}{2\alpha} \int_m^{t_1} r^3 \, dr + \frac{\pi}{2\alpha} m^2 \int_m^{t_1} r \, dr \\ &= \pi k t_1^2 \ln \frac{t_1}{m} + \frac{\pi}{2} \underbrace{\left(\frac{m^2}{2\alpha} - \frac{k}{m} \right)}_{\leq 0} (t_1^2 - m^2) + \frac{\pi}{8\alpha} \underbrace{(m^4 - t_1^4)}_{\leq 0} \\ &\leq \frac{\pi t_1^4}{2\alpha} m \ln \frac{t_1}{m} \leq \frac{\pi t_1^4}{2\alpha} \ln \frac{t_1}{m} = \underbrace{\frac{\pi t_1^4}{2\alpha}}_{=: C_1(\alpha)} \ln m^{-1} + \underbrace{\frac{\pi t_1^4}{2\alpha}}_{=: C_2(\alpha)} \ln t_1. \end{aligned}$$

□

Lemma A.3. We have, for m in $(0, t_1)$,

$$C_1(\alpha) \ln(m^{-1}) - C_2(\alpha) \leq \theta(m),$$

where C_1 and C_2 are constants depending on α .

Proof. We fix $n \in \mathbb{N}$ and $(x_i)_{i=1, \dots, n} \in I^2$. We consider the sets $K_m := \bigcup_{i=1}^n \overline{B(x_i, mn^{-1/2})}$ and $U_m := I^2 \setminus K_m$. Let us denote u_m^1 the solution of Problem 3.1 with $g = 1$, $K = K_m$ and $D = I^2$. Using Holder inequality we have

$$\left(\int_{\partial U_m} \frac{\partial u_m^1}{\partial n} \, d\mathcal{H}^1 \right)^2 \leq \int_{\partial U_m} \left| \frac{\partial u_m^1}{\partial n} \right|^2 \, d\mathcal{H}^1 \times \int_{\partial U_m} \, d\mathcal{H}^1 = \mathcal{H}^1(\partial U_m) \int_{\partial U_m} \left| \frac{\partial u_m^1}{\partial n} \right|^2 \, d\mathcal{H}^1.$$

Moreover, we have thanks to the Green formula

$$\int_{\partial U_m} \frac{\partial u_m^1}{\partial n} \, d\mathcal{H}^1 = \int_{U_m} \Delta u_m^1 \, dx = \frac{1}{\alpha} \int_{U_m} (u_m^1 - 1) \, dx = \frac{1}{\alpha} \|u_m^1\|_{L^1(U_m)} - \frac{1}{\alpha} |U_m|.$$

Thus

$$\begin{aligned} \left(\frac{1}{\alpha} \|u_m^1\|_{L^1(U_m)} - \frac{1}{\alpha} |U_m| \right)^2 &\leq \mathcal{H}^1(\partial U_m) \int_{\partial U_m} \left| \frac{\partial u_m^1}{\partial n} \right|^2 \, d\mathcal{H}^1 \\ \Leftrightarrow \frac{1}{\alpha^2} |U_m|^2 - \frac{2}{\alpha^2} \|u_m^1\|_{L^1(U_m)} |U_m| &\leq \mathcal{H}^1(\partial U_m) \int_{\partial U_m} \left| \frac{\partial u_m^1}{\partial n} \right|^2 \, d\mathcal{H}^1. \end{aligned}$$

The fact that $|U_m| \geq 1 - 2\pi m^2$ and Property A.1 give us

$$\frac{2\pi^2\alpha - 1}{\alpha^2(1 + 2\pi^2\alpha)} - \frac{2\pi}{\alpha^2}m \leq \mathcal{H}^1(\partial U_m) \int_{\partial U_m} \left| \frac{\partial u_m^1}{\partial n} \right|^2 d\mathcal{H}^1.$$

Also, it holds $\mathcal{H}^1(\partial U_m) \leq 2\pi m\sqrt{n}$. Then

$$\begin{aligned} \frac{2\pi^2\alpha - 1}{\alpha^2(1 + 2\pi^2\alpha)} - \frac{2\pi}{\alpha^2}m &\leq 2\pi m\sqrt{n} \int_{\partial U_m} \left| \frac{\partial u_m^1}{\partial n} \right|^2 d\mathcal{H}^1 \\ \Leftrightarrow \frac{2\pi^2\alpha - 1}{2\pi\alpha^2(1 + 2\pi^2\alpha)} \frac{1}{m} - \frac{1}{\alpha^2} &\leq \sqrt{n} \int_{\partial U_m} \left| \frac{\partial u_m^1}{\partial n} \right|^2 d\mathcal{H}^1. \end{aligned}$$

Using that $-\frac{dF}{dm} = \sqrt{n}^{-1} \int_{\partial U_m} \left| \frac{\partial u_m^1}{\partial n} \right|^2 d\mathcal{H}^1$, we have

$$\frac{2\pi^2\alpha - 1}{2\pi\alpha^2(1 + 2\pi^2\alpha)} \frac{1}{m} - \frac{1}{\alpha^2} \leq -n \frac{dF}{dm}.$$

Integrating over $[m_1, m_2] \subset (0, t_1)$ yields to

$$\frac{2\pi^2\alpha - 1}{2\pi\alpha^2(1 + 2\pi^2\alpha)} \ln\left(\frac{m_2}{m_1}\right) - \frac{m_2 - m_1}{\alpha^2} + nF_{m_2} \leq nF_{m_1}.$$

Taking inf over x_i and passing to lim inf over n when n tends to $+\infty$ leads to

$$\frac{2\pi^2\alpha - 1}{2\pi\alpha^2(1 + 2\pi^2\alpha)} \ln\left(\frac{m_2}{m_1}\right) - \frac{m_2 - m_1}{\alpha^2} + \theta(m_2) \leq \theta(m_1).$$

In particular, if $m_2 = t_1$ and $m_1 = m$, $0 < m < t_1 = \frac{\sqrt{2}}{2}$,

$$\begin{aligned} &\frac{2\pi^2\alpha - 1}{2\pi\alpha^2(1 + 2\pi^2\alpha)} \ln\left(\frac{t_1}{m}\right) - \frac{t_1 - m}{\alpha^2} \leq \theta(m) \\ \Leftrightarrow &\frac{2\pi^2\alpha - 1}{2\pi\alpha^2(1 + 2\pi^2\alpha)} \ln\left(\frac{t_1}{m}\right) - \frac{t_1}{\alpha^2} \leq \theta(m) \\ \Leftrightarrow &\underbrace{\frac{2\pi^2\alpha - 1}{2\pi\alpha^2(1 + 2\pi^2\alpha)} \ln(m^{-1})}_{=: C_1(\alpha)} - \underbrace{\left(\frac{2\pi^2\alpha - 1}{2\pi\alpha^2(1 + 2\pi^2\alpha)} \ln(t_1^{-1}) + \frac{t_1}{\alpha^2}\right)}_{=: C_2(\alpha)} \leq \theta(m). \end{aligned}$$

□

B Asymptotic Development Calculus

Let x_0 be in \mathbb{R}^2 and $\varepsilon > 0$. In this section, we aim to find an estimate of

$$\int_{B(x_0, \varepsilon)} w \, dx,$$

where w the solution of the problem below :

Problem B.1. Find w in $H_0^1(B(x_0, \varepsilon))$ such that

$$\begin{cases} w - \alpha \Delta w = g, & \text{in } B(x_0, \varepsilon), \\ w = 0, & \text{on } \partial B(x_0, \varepsilon). \end{cases} \quad (15)$$

We did not find this result in the literature despite it may exist. For the sake of completeness, we propose a way to find this estimate. To solve Problem B.1, we use Green functions $G : B(x_0, \varepsilon) \times B(x_0, \varepsilon)$, corresponding to Problem B.1 which are solution to

Problem B.2. Find $G(\cdot, y)$ in $H_0^1(B(x_0, \varepsilon))$ such that

$$\begin{cases} G(x, y) - \alpha \Delta_x G(x, y) = \delta_y(x), & x \in B(x_0, \varepsilon), \\ G(x, y) = 0, & x \in \partial B(x_0, \varepsilon), \end{cases} \quad (16)$$

for y in $B(x_0, \varepsilon)$.

We have,

Proposition B.1. Let G be Green functions corresponding to Problem B.2. Then, for x in $\overline{B(x_0, \varepsilon)}$,

$$w(x) := \int_{B(x_0, \varepsilon)} g(y) G(x, y) \, dy,$$

is the solution of Problem B.1.

Proof. Let x be in $B(x_0, \varepsilon)$.

$$\begin{aligned} w(x) - \alpha \Delta w(x) &= \int_{B(x_0, \varepsilon)} g(y) G(x, y) \, dy - \alpha \int_{B(x_0, \varepsilon)} g(y) \Delta_x G(x, y) \, dy \\ &= \int_{B(x_0, \varepsilon)} g(y) (G(x, y) - \alpha \Delta_x G(x, y)) \, dy \\ &= \int_{B(x_0, \varepsilon)} g(y) \delta_y(x) \, dy \\ &= g(x). \end{aligned}$$

Moreover, we have, $w(x) = 0$, for x on $\partial B(x_0, \varepsilon)$. □

From now, our goal is to find Green functions G . To do so, we write G as the sum of a particular solution G_p of Problem B.2 without the boundary condition, and the general solution G_0 of the homogeneous version of Problem B.2 such that $G_0 = -G_p$ on $\partial B(x_0, \varepsilon)$. Below is the main proposition of this section,

Proposition B.2. We have when ε tends to 0,

$$\int_{B(x_0, \varepsilon)} w(x) \, dx = -g(x_0) \pi \varepsilon^4 \ln(\varepsilon) + O(\varepsilon^4).$$

Proof. For ε small enough, we have, using Proposition B.1,

$$\int_{B(x_0, \varepsilon)} w(x) dx = \int_{B(x_0, \varepsilon)} \int_{B(x_0, \varepsilon)} g(y) G(x, y) dy dx.$$

Using Fubini, we get

$$\begin{aligned} \int_{B(x_0, \varepsilon)} w(x) dx &= \int_{B(x_0, \varepsilon)} g(y) \int_{B(x_0, \varepsilon)} G(x, y) dx dy \\ &= \int_{B(x_0, \varepsilon)} g(y) \int_{B(x_0, \varepsilon)} G_p(x, y) dx dy + \int_{B(x_0, \varepsilon)} g(y) \int_{B(x_0, \varepsilon)} G_0(x, y) dx dy. \end{aligned}$$

Proposition B.4 and Proposition B.5 give us the result. \square

It remains to state and to prove Proposition B.4 and Proposition B.5. We start by giving an explicit expression for G_p with the following proposition.

Proposition B.3. For x and y in $B(x_0, \varepsilon)$ such that $x \neq y$, we have

$$G_p(x, y) = \frac{1}{2\pi} K_0\left(\frac{1}{\sqrt{\alpha}}|x - y|\right),$$

where K_0 is the modified Bessel function of the second kind, see [41].

Proof. See [42]. \square

Then, we compute the first part of Proposition B.2.

Proposition B.4. When ε tends to 0, we have,

$$\int_{B(x_0, \varepsilon)} g(y) \int_{B(x_0, \varepsilon)} G_p(x, y) dx dy = -g(x_0) \frac{\pi}{2} \varepsilon^4 \ln(\varepsilon) + O(\varepsilon^4).$$

Proof. According to [41], we have the following asymptotic development

$$K_0(z) = -\ln z + \ln 2 - \gamma + O(z^2 |\ln z|),$$

for $z \rightarrow 0$, where γ denotes the Euler–Mascheroni constant. Then,

$$G_p(x, y) = -\frac{1}{2\pi} \left(\ln|x - y| + \frac{1}{2} \ln \alpha + \ln 2 - \gamma \right) + O(|x - y|^2 |\ln|x - y||),$$

for $|x - y| \rightarrow 0$. Thus,

$$\begin{aligned} \int_{B(x_0, \varepsilon)} g(y) \int_{B(x_0, \varepsilon)} G_p(x, y) dx dy &= -\frac{1}{2\pi} \int_{B(x_0, \varepsilon)} g(y) \int_{B(x_0, \varepsilon)} \ln|x - y| dx dy \\ &\quad - \left(\frac{1}{2} \ln \alpha + \ln 2 - \gamma \right) \frac{\varepsilon^2}{2} \int_{B(x_0, \varepsilon)} g(y) dy + O(1) \int_{B(x_0, \varepsilon)} g(y) \int_{B(x_0, \varepsilon)} |x - y|^2 |\ln|x - y|| dx dy. \end{aligned}$$

Using Taylor's formula, we have

$$\begin{aligned}
& \int_{B(x_0, \varepsilon)} g(y) \int_{B(x_0, \varepsilon)} G_p(x, y) dx dy = -\frac{1}{2\pi} g(x_0) \int_{B(x_0, \varepsilon)} \int_{B(x_0, \varepsilon)} \ln|x-y| dx dy \\
& \quad + O(1) \int_{B(x_0, \varepsilon)} \|y-x_0\| \int_{B(x_0, \varepsilon)} \ln|x-y| dx dy - \left(\frac{1}{2} \ln \alpha + \ln 2 - \gamma\right) \frac{\pi}{2} g(x_0) \varepsilon^4 + O(\varepsilon^4) \\
& \quad + O(1) \int_{B(x_0, \varepsilon)} \int_{B(x_0, \varepsilon)} |x-y|^2 \ln|x-y| dx dy + O(1) \int_{B(x_0, \varepsilon)} \|y-x_0\| \int_{B(x_0, \varepsilon)} |x-y|^2 \ln|x-y| dx dy \\
\leq & -\frac{1}{2\pi} g(x_0) \int_{B(x_0, \varepsilon)} \int_{B(x_0, \varepsilon)} \ln(2\varepsilon) dx dy + O(1) \int_{B(x_0, \varepsilon)} \|y-x_0\| \int_{B(x_0, \varepsilon)} \ln(2\varepsilon) dx dy \\
& - \left(\frac{1}{2} \ln \alpha + \ln 2 - \gamma\right) \frac{\pi}{2} g(x_0) \varepsilon^4 + O(\varepsilon^4) \\
& + O(1) \int_{B(x_0, \varepsilon)} \int_{B(x_0, \varepsilon)} |x-y|^2 \ln(2\varepsilon) dx dy + O(1) \int_{B(x_0, \varepsilon)} \|y-x_0\| \int_{B(x_0, \varepsilon)} |x-y|^2 \ln(2\varepsilon) dx dy \\
= & -\frac{\pi}{2} g(x_0) \varepsilon^4 \ln(2\varepsilon) + O(\varepsilon^5 \ln(2\varepsilon)) - \left(\frac{1}{2} \ln \alpha + \ln 2 - \gamma\right) \frac{\pi}{2} g(x_0) \varepsilon^4 + O(\varepsilon^4) + O(\varepsilon^6 \ln(2\varepsilon)) + O(\varepsilon^7 \ln(2\varepsilon)) \\
= & -\frac{\pi}{2} g(x_0) \varepsilon^4 \ln(\varepsilon) + O(\varepsilon^5 \ln(\varepsilon)) - \left(\frac{1}{2} \ln \alpha - \gamma\right) \frac{\pi}{2} g(x_0) \varepsilon^4 + O(\varepsilon^4) + O(\varepsilon^6 \ln(\varepsilon)) + O(\varepsilon^7 \ln(\varepsilon)) \\
= & -\frac{\pi}{2} g(x_0) \varepsilon^4 \ln(\varepsilon) + O(\varepsilon^4).
\end{aligned}$$

□

And we finish by computing the second part of Proposition B.2.

Proposition B.5. *When ε tends to 0, we have,*

$$\int_{B(x_0, \varepsilon)} g(y) \int_{B(x_0, \varepsilon)} G_0(x, y) dx dy = -g(x_0) \frac{\pi}{2} \varepsilon^4 \ln \varepsilon + O(\varepsilon^4).$$

Proof. We start by using Taylor's formula on g around x_0 ,

$$\begin{aligned}
& \int_{B(x_0, \varepsilon)} g(y) \int_{B(x_0, \varepsilon)} G_0(x, y) dx dy = g(x_0) \int_{B(x_0, \varepsilon)} \int_{B(x_0, \varepsilon)} G_0(x, y) dx dy \\
& \quad + O(1) \int_{B(x_0, \varepsilon)} \|y-x_0\| \int_{B(x_0, \varepsilon)} G_0(x, y) dx dy \\
\leq & g(x_0) \pi \varepsilon^2 \int_{B(x_0, \varepsilon)} \|G_0(\cdot, y)\|_{L^\infty(B(x_0, \varepsilon))} dy + O(\varepsilon^2) \int_{B(x_0, \varepsilon)} \|y-x_0\| \|G_0(\cdot, y)\|_{L^\infty(B(x_0, \varepsilon))} dy.
\end{aligned}$$

Since G_0 satisfies the maximum principle [39],

$$\begin{aligned}
& \int_{B(x_0, \varepsilon)} g(y) \int_{B(x_0, \varepsilon)} G_0(x, y) dx dy \leq g(x_0) \pi \varepsilon^2 \int_{B(x_0, \varepsilon)} \|G_0(\cdot, y)\|_{L^\infty(\partial B(x_0, \varepsilon))} dy \\
& \quad + O(\varepsilon^2) \int_{B(x_0, \varepsilon)} \|y-x_0\| \|G_0(\cdot, y)\|_{L^\infty(\partial B(x_0, \varepsilon))} dy \\
= & g(x_0) \pi \varepsilon^2 \int_{B(x_0, \varepsilon)} \|G_p(\cdot, y)\|_{L^\infty(\partial B(x_0, \varepsilon))} dy + O(\varepsilon^2) \int_{B(x_0, \varepsilon)} \|y-x_0\| \|G_p(\cdot, y)\|_{L^\infty(\partial B(x_0, \varepsilon))} dy \\
= & g(x_0) \frac{1}{2} \varepsilon^2 \int_{B(x_0, \varepsilon)} \left\| K_0\left(\frac{1}{\sqrt{\alpha}}|\cdot-y|\right) \right\|_{L^\infty(\partial B(x_0, \varepsilon))} dy + O(\varepsilon^2) \int_{B(x_0, \varepsilon)} \|y-x_0\| \left\| K_0\left(\frac{1}{\sqrt{\alpha}}|\cdot-y|\right) \right\|_{L^\infty(\partial B(x_0, \varepsilon))} dy.
\end{aligned}$$

According to [41], K_0 is an increasing function. Thus, for y in $B(x_0, \varepsilon)$,

$$\left\| K_0\left(\frac{1}{\sqrt{\alpha}}|\cdot - y|\right) \right\|_{L^\infty(\partial B(x_0, \varepsilon))} := \sup_{x \in \partial B(x_0, \varepsilon)} \left| K_0\left(\frac{1}{\sqrt{\alpha}}|x - y|\right) \right|,$$

is attained where $|x - y| := \sqrt{r_x^2 + r_y^2 - 2r_x r_y \cos(\theta_x - \theta_y)}$ is maximal, i.e. when $\cos(\theta_x - \theta_y) = -1$, i.e. for $\theta_x = \pi + \theta_y$. In that case,

$$|x - y| = \sqrt{\varepsilon^2 + r_y^2 + 2\varepsilon r_y} = \varepsilon + r_y.$$

Thus,

$$\|G_p(\cdot, y)\|_{L^\infty(\partial B(x_0, \varepsilon))} = \frac{1}{2\pi} K_0\left(\frac{1}{\sqrt{\alpha}}(\varepsilon + r_y)\right).$$

Then, we have

$$\begin{aligned} \int_{B(x_0, \varepsilon)} g(y) \int_{B(x_0, \varepsilon)} G_0(x, y) dx dy &\leq g(x_0) \pi \varepsilon^2 \int_0^\varepsilon r_y K_0\left(\frac{1}{\sqrt{\alpha}}(\varepsilon + r_y)\right) dy + O(\varepsilon^2) \int_0^\varepsilon r_y^2 K_0\left(\frac{1}{\sqrt{\alpha}}(\varepsilon + r_y)\right) dy \\ &\leq g(x_0) \frac{\pi}{2} \varepsilon^4 K_0\left(\frac{2\varepsilon}{\sqrt{\alpha}}\right) + O(\varepsilon^5) K_0\left(\frac{2\varepsilon}{\sqrt{\alpha}}\right). \end{aligned}$$

Again, we use that, when z tends to 0,

$$K_0(z) = -\ln z + \ln 2 - \gamma + O(z^2 |\ln z|),$$

and get, since ε tends to 0,

$$K_0\left(\frac{2\varepsilon}{\sqrt{\alpha}}\right) = -\ln \varepsilon + \frac{1}{2} \ln \alpha - \gamma + O(\varepsilon^2 |\ln \varepsilon|).$$

Therefore,

$$\begin{aligned} \int_{B(x_0, \varepsilon)} g(y) \int_{B(x_0, \varepsilon)} G_0(x, y) dx dy &\leq -g(x_0) \frac{\pi}{2} \varepsilon^4 \ln \varepsilon + g(x_0) \frac{\pi}{4} \varepsilon^4 \ln \alpha - g(x_0) \frac{\pi}{2} \varepsilon^4 \gamma + O(\varepsilon^5 \ln \varepsilon) \\ &= -g(x_0) \frac{\pi}{2} \varepsilon^4 \ln \varepsilon + O(\varepsilon^4). \end{aligned}$$

□

C Algorithms

Here, we present and discuss algorithms used in Section 5. Each algorithm is used during the encoding step and gives an inpainting mask K subset of D . The input data f is the image to compress, δt is the time-step of the parabolic inpainting discretization, Section 4, $\alpha > 0$ and c is the percentage amount of pixels in the mask i.e. the percentage amount of pixels to save. We denote in the sequel for a discrete mask A in D , $\#A$, the number of pixels in A .

C.1 L2Dec Method

For this method, we want, for n in $\{0, \dots, N\}$, $K_{n+1} \subset K_n$. The parameter N in \mathbb{N}^* is the number of time-step we want to compute. Thus, we compute the solution u of Problem 4.1 for $t = N\delta t\alpha$. For each step n in $\{0, \dots, N\}$, we set K_n as the thresholding of $\mathbf{1}_{K_{n-1}}(f - \delta t\alpha\Delta f - u^n)^2$ such that $\#K_n \leq \#K_{n-1}$. The term $\mathbf{1}_{K_{n-1}}$ ensure us that K_n is a subset of K_{n-1} . Then, we compute u^{n+1} , solution of Problem 4.2 with u^n , f and K_n . We compare two choices for u_0 . We start when $u_0 = 0$. Thus, K_0 is the thresholding of $(f - \delta t\alpha\Delta f)^2$. It corresponds to the stationary case, Section 2. Then, when $u_0 = f$, K_0 is the thresholding of $(\Delta f)^2$. In that case, δt and α do not have any influence on the output mask K_N given by the method. Indeed, since every K_n is a subset of K_{n-1} , the resulting mask will be the same as the H^1 one proposed in [17] since $u_n = f$ in K_{n-1} . Figure 9 is results for the two cases when $N = 50$ and $c = 0.1$.

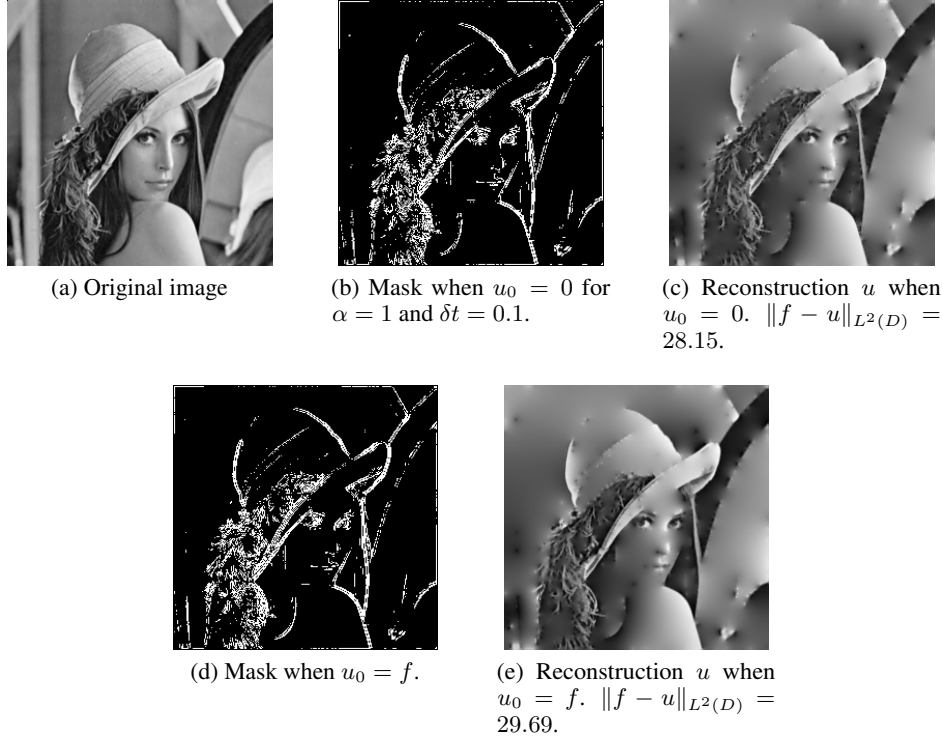


Figure 9: Initial condition comparison for “L2Dec” method.

C.2 L2Inc Method

Now, we present the “L2Inc” method. Unlike the “L2Dec” method, we want $K_{n-1} \subset K_n$ for n in $\{0, \dots, N\}$, N in \mathbb{N}^* . For each step n in $\{0, \dots, N\}$, we set K_n as the union of K_{n-1} and the thresholding of $(1 - \mathbf{1}_{K_{n-1}})(f - \delta t\alpha\Delta f - u^n)^2$. Therefore, we have $\#K_n \geq \#K_{n-1}$. The term $(1 - \mathbf{1}_{K_{n-1}})$ ensure us to not add to K_n pixels that are already in K_{n-1} . Then, we compute u^{n+1} , solution of Problem 4.2 with u^n , f and K_n . Again, we have to chose the initial condition u_0 . We propose and compare two choices for u_0 . When $u_0 = 0$, K_0 corresponds to the stationary case, Section 2. When $u_0 = f$, K_0 is the “H1” mask. Figure 10 is results for the two cases when $N = 40$, $\delta t = 0.1$, $\alpha = 20$ and $c = 0.1$.

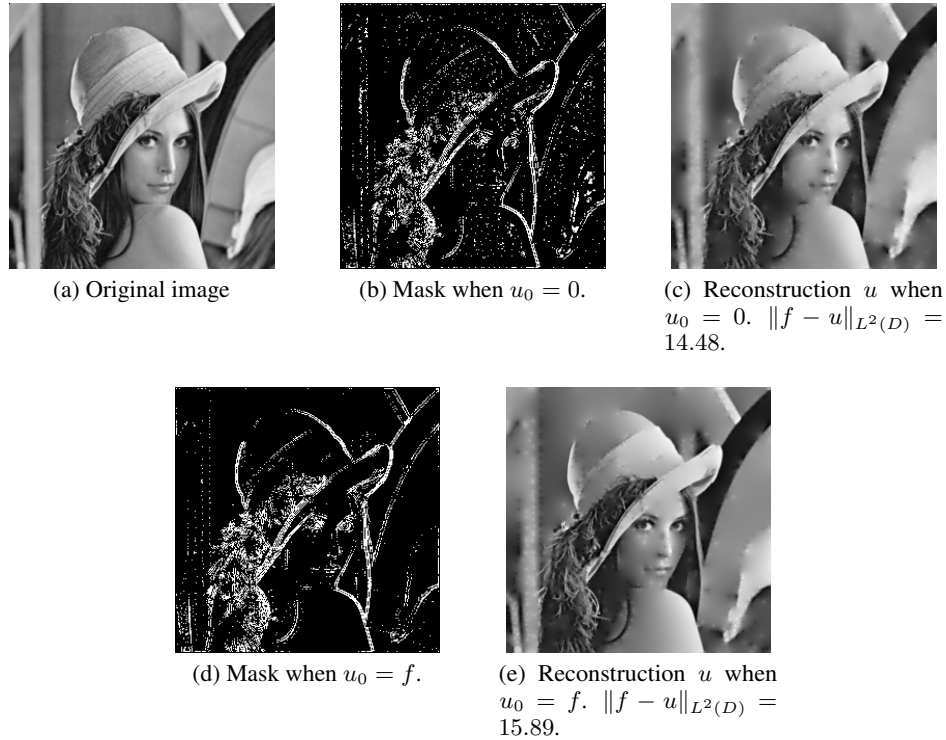


Figure 10: Initial condition comparison for “L2Inc” method.

C.3 L2Insta Method

Finally, we propose a last time-dependent method : the “L2Insta” method. Here, we do not impose sets to be included into others, but we still want $\#K_n = \#K_{n-1}$. For each step n in $\{0, \dots, N\}$, K_n is the halftoning of $(f - \delta t \alpha \Delta f - u^n)^2$. Then, we compute u^{n+1} , solution of Problem 4.2 with u^n , f and K_n . Again, we have to chose the initial condition u_0 . We propose and compare two choices for u_0 . When $u_0 = 0$, K_0 corresponds to the stationary case, Section 2. When $u_0 = f$, K_0 is the “H1” mask. Figure 11 is results for the two cases when $N = 10$, $\delta t = 0.1$, $\alpha = 10$ and $c = 0.1$.

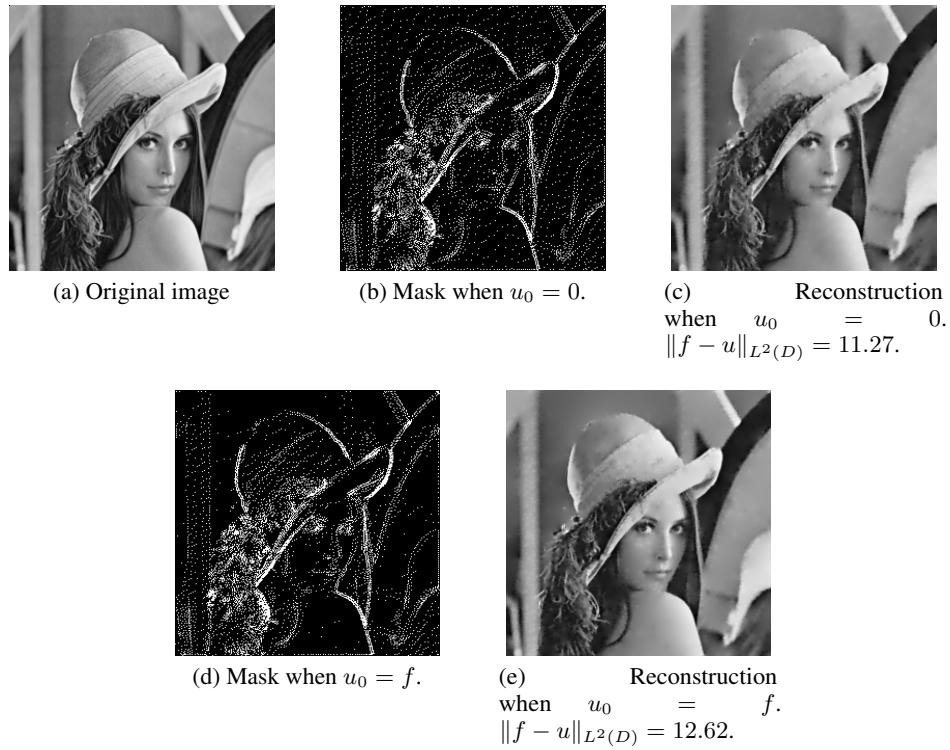


Figure 11: Initial condition comparison for “L2Insta” method.

For our three methods, the choice $u_0 = 0$ seems to be the best one. That is why we will use this initial condition for our experiments.